Optimisation of water, temperature and voltage management on a regenerative fuel cell

Petrus Jacobus Malan van Tonder

210125063

A dissertation submitted in fulfillment of the requirements for the Magister Technologiae: Engineering: Electrical

Department: Electronic Engineering

Faculty of Engineering and Technology

Vaal University of Technology

Vanderbijlpark

Supervisor: Prof HCvZ Pienaar

Date: December 2011

Declaration

I, Malan van Tonder hereby declare that the following research information is solely my own work. This is submitted in fulfillment of the requirements for the Magister Technologiae: Engineering: Electrical to the Department of Electronic Engineering at the Vaal University of Technology, Vanderbijlpark. It has not been submitted before for any assessment to any educational institution.

……
Malan van Tonder

Date: ……..

Acknowledgements

I hereby wish to express my gratitude to the following individuals who enabled this document to be completed successfully:

- Prof HCvZ Pienaar for encouragement and guidance throughout this research
- Telkom Centre of Excellence, TFMC, M-Tech an THRIP
- Personnel of the Department of Electronic Engineering for support and encouragement

Dedication

This dissertation is dedicated to my parents, Pieter and Annalize, and to my sister, Liezl, for their support and encouragement during the study of this project.

The winds of God are always blowing, but you must set the sails – unknown.

Abstract

“Never before in peacetime have we faced such serious and widespread shortage of energy” according to John Emerson, an economist and power expert for Chase Manhattan Bank. Many analysts believe that the problem will be temporary, but others believe the energy gap will limit economic growth for years to come. A possible solution to this problem can be fuel cell technology. Fuel cells (FCs) are energy conversion devices that generate electricity from a fuel like hydrogen. The FC however, could also be used in the reverse or regenerative mode to produce hydrogen.

The reversible fuel cell (RFC) can produce hydrogen and oxygen by introducing water to the anode electrode chamber, and applying a potential across the anode and cathode. This will cause the decomposition of the water to produce oxygen at the anode side and hydrogen at the cathode side. In order to make this process as efficient as possible several aspects need to be optimised, for example, the operation temperature of the RFC, water management inside the RFC and supply voltage to the RFC.

A three cell RFC and its components were constructed. The three cell RFC was chosen owing to technical reasons. The design factors that were taken into consideration were the different types of membranes, electrocatalysts, bipolar plates and flow topologies. A water trap was also designed and constructed to eliminate the water from the hydrogen water mixture due to water crossover within the MEA. In order to optimise the operation of the RFC a number of experiments were done on the RFC. These experiments included the optimal operating voltage, the effect that the temperature has on the production rate of hydrogen, and the effect that the water flow through the RFC has on the production rate of hydrogen.

It was found that there is no need to control the water flow through the RFC because it had no effect on the production rate of hydrogen. The results also showed that if the operating temperature of the RFC were increased, the energy it consumes to warm the RFC significantly decreases the efficiency of the whole system. Thus the RFC need not be heated because it consumes significantly more energy to heat the RFC compared to the energy available from the hydrogen produced for later use. The optimised operating voltage for the three cell RFC was found to be 5.05 V. If the voltage were to be increased or decreased the RFC efficiency would decrease.

Table of contents

Declaration ii
Acknowledgements iii
Dedication iv
Abstract v
List of Figures viii
List of tables x
Glossary of abbreviations and definitions xi

CHAPTER 1 – Introduction and overview

1.1 Background 1
1.2 Regenerative fuel cells 2
1.3 Problem statement 2
1.4 Justification for the research: The imperatives 2
1.5 Aims 4
1.6 Research methodology 4
1.7 Delimitation 5
1.8 Overview of the report 5
1.9 Summary 5

CHAPTER 2 – Regenerative fuel cells

2.1 History of the RFC 6
2.2 Different methods to generate hydrogen 6
2.3 Operation of a RFC 8
2.4 Components of the RFC 9
2.4.1 MEA 9
2.4.2 Proton exchange membrane 10
2.4.3 Electrocatalyst 11
2.4.4 Bipolar plates 13
2.4.4.1 Plate materials 14
2.4.4.2 Flow field designs 16
2.5 Chemical thermodynamics 19
2.6 The HOGEN GC hydrogen generator 22
2.7 Water 23
2.8 Effect of the temperature on the RFC 24

2.4 Summary 24

CHAPTER 3 - Design of the three cell RFC

3.1 Introduction 26
3.2 Bipolar plates 26
3.3 Membrane Electrode Assembly (MEA) 30
3.4 Final stack assembly 30
3.5 Water crossover 31
3.6 Water trap 32
3.7 PLC 34
3.8 Summary 34

CHAPTER 4 - Measurements and results

4.1 Introduction 36
4.2 Experimental setup 36
4.3 Stack voltage 41
4.4 Water supply 46
4.5 The effect of temperature on the RFC 49
4.5.1 Nexa® Power Module 54
4.6 The optimised RFC system 56
4.7 Summary 59

CHAPTER 5 – Conclusions and recommendations

5.1 Conclusions 61
5.1.1 The construction of the RFC 61
5.1.2 Control aspects of the RFC 62
5.2 Recommendations 63

BIBLIOGRAPHY 64

ANNEXURES PAGE NUMBERS 68

List of Figures

Figure 1:	a RFC in the fuel cell mode and electrolyser mode	3
Figure 2:	Solar hydrogen system	4
Figure 3:	Block diagram of a typical RFC	8
Figure 4:	Operation of a RFC	8
Figure 5:	Basic structure of the RFC	9
Figure 6:	Nafion structure	10
Figure 7:	Bipolar plates	13
Figure 8:	Mass distribution in 33 kW PEMFC stack	16
Figure 9:	Pin type	17
Figure 10:	Straight and parallel channel type	18
Figure 11:	Single continuous serpentine	18
Figure 12:	Several continuous serpentine	18
Figure 13:	Integrated channel flow type	19
Figure 14:	HOGEN GC hydrogen generator	22
Figure 15:	HOGEN GC block diagram	23
Figure 16:	Effects of temperature on the RFC	24
Figure 17:	RFC block diagram	26
Figure 18:	Anode flow field plate	28
Figure 19:	Cathode flow field plate	29
Figure 20:	Middle bipolar plate	29
Figure 21:	Nafion N-115 MEA	30
Figure 22:	Exploded view of RFC	30
Figure 23:	Complete three cell RFC stack	31
Figure 24:	Water trap design	33
Figure 25:	Water trap with valve	33
Figure 26:	Water trap built into the RFC test rig	34
Figure 27:	Block diagram of the experimental setup	36
Figure 28:	RFC and the water trap	37
Figure 29:	Indirect tank-in-tank water heating	38
Figure 30:	Temperature controller	38
Figure 31:	Element circuit	39
Figure 32:	Water supply to the RFC	39
Figure 33:	Ritter flow meter	40
Figure 34:	Stack voltage experimental setup	42
Figure 35:	Flow of H_2 and current vs. stack voltage	44

Figure 36:	Efficiency and current vs. voltage of the RFC	45
Figure 37:	Water supply experimental setup	46
Figure 38:	Pump supply voltage vs. flow rate of H_2O	47
Figure 39:	Flow rate of H_2 and pump voltage vs. flow rate of H_2O produced	48
Figure 40:	Temperature experimental setup	50
Figure 41:	Current vs. temperature	51
Figure 42:	Flow of H_2 produced vs. temperature	52
Figure 43:	Nexamon® OEM control software	54
Figure 44:	Experiment setup with Nexa ® Power Module	55
Figure 45:	PLC control block diagram	57
Figure 46:	Relay Codesys programming	58
Figure 47:	Visual form	58
Figure 48:	Water release valve Codesys programming	58
Figure 49:	Water release valve output wave form	59
Figure 50:	Hydrogen generator	59

List of tables

Table 1:	Types of electrolysers	7
Table 2:	Various membranes and their applications	11
Table 3:	Nafion membrane thickness	11
Table 4:	Flow topologies	27
Table 5:	Ritter specifications	41
Table 6:	Stack voltages	43
Table 7:	RFC efficiency data	45
Table 8:	Relationship between pump supply voltage and H_2O flow rate	47
Table 9:	Flow rate of H_2O vs. flow rate of H_2 produced	49
Table 10:	Effects of temperature	51
Table 11:	Hydrogen consumption	55
Table 12:	Energy that is generated by the extra hydrogen	56

Glossary of abbreviations and definitions

A

A – Amp
AC – Alternating current
mA/mm^{-2} – Milliamp per square millimeter

C

CFC – Continuous function chart
CO_2 – Carbon dioxide
CO – Carbon monoxide
CCM – Catalyst-Coated Membrane
°C – Degree Celsius
c_p – Heat constant
cm^2 – Square centimetre

D

DME – Department of mineral and energy
DC – Direct current
DMFC – Direct methanol fuel cell

E

η^E – Efficiency of EFC
E – Electrolyser
e^- – Electron
E^o – Reversible voltage
E^{tn} – Thermoneutral

F

F – Faradays constant
FC – Fuel cell
FBD – Function block diagram

G

ΔG – Gibbs standard free energy
$\mu g/mm^3$ – micro gram per square millimeter

H

ΔH – Enthalpy value of reaction
H^+ – Hydrogen proton
H_2 – Hydrogen gas molecule
H_3O – Hydronium ions
HVV – Higher heating value
h – Hour
H_2O – Water

I

l/h – liter per hour
IL – Instruction list
Ir – Iridium
IrO_2 – Iridium oxide
$IrRuO_2$ – Iridium ruthenium oxide

J

J – Joule

K

K – Kelvin
kW – Kilowatt
KJ – Kilojoule
kPa – Kilopascal

L

l/min – litre per minute
l/h – litre per hour
LD – Ladder diagram
ml/min – millilitre per minute

M

m – gradient
MEA – Membrane Electrode Assembly
um – micrometer
mm – Millimeter
min – Minute
MCFC – Molten Carbonate Fuel Cell

O

O_2 – Oxygen
O^+ – Oxygen protons

P

Pt – Platinum
PAFC – Phosphoric Acid Fuel Cell
PLC – Programmable Logic Controller
PEMFC – Proton Exchange Membrane Fuel Cell

Q,R

Q – Amount of power (KJ)
R – Universal gas constant
RFC – Regenerative Fuel Cell
Ru – Ruthenium

S

ΔS – Entropy
SFC – Sequential function charts
$S.mm^{-1}$ – Siemens per millimetre
SHS – Solar hydrogen system
STP – Standard Temperature and Pressure
ST – Structured text

T

T – Absolute Temperature (K)
*d*T – Temperature difference
TCD – Thermal Conductivity Detector
t – Time

V

V_{H2} – Flow rate in mole
V – Volts

W

W – Watt
$W.mm^{-1}$ – Watt per millimetre
W.h – Watt hour
Wt.% – Weight percentage

Chapter 1 Introduction and overview

1.1 Background

“Never before in peacetime have we faced such a serious and widespread shortage of energy” according to John Emerson, an economist and power expert for Chase Manhattan Bank. Many analysts believe that the problem will be temporary, but others believe the energy gap will limit economic growth for years to come (van Tonder and Pienaar, 2010).

Fuel cells (FCs) are energy conversion devices that generate electricity from fuel. The FC belongs to the family of batteries, known as ‘electrochemical batteries’. The FC, however, is not a battery because it generates electricity through reactants stored externally in comparison to that of a battery that stores the chemical reactants internally. When the chemical energy has been converted to electrical energy in a battery, it must be thrown away (primary battery) or recharged appropriately (secondary / rechargeable battery). However, FCs oxidise externally supplied fuel and therefore do not have to be recharged. A FC uses a chemical reaction to provide an external voltage (Moorthy, 2006).

Various types of FCs have been developed to generate power according to the applications and load requirements. These fuel cells are normally distinguished by the electrolyte used, although the construction of the electrodes (fuel cell hardware) is also different in each (Moorthy, 2006). The most popular FCs are discussed below:

- **Direct Methanol Fuel Cells (DMFC)** - The direct methanol fuel cell is a low temperature fuel cell that operates in a temperature range between 0°C and 60°C. In order for the fuel cell to supply the user with power a methanol water mixture and oxygen must be supplied to the fuel cell. The by-product is pure water and heat. The advantage of the fuel cell is quick startup time, high energy density, no reforming needed, etc. The disadvantages of the cells are fuel crossover and safety concerns, etc. (Basu, 2007:5).

- **Proton Exchange Membrane Fuel Cells (PEMFC)** - These fuel cells operate at relatively low temperatures between 20°C and 100°C. In order to generate power with this fuel cell, hydrogen and oxygen must be supplied to the fuel cell and the by-product is water and heat. The advantage of this type of fuel cell is its relative small size and relatively high power density. It can also vary its output quickly to meet shifts in power demands (Basu, 2007:5).

- **Phosphoric Acid Fuel Cell (PAFC)** - This type of fuel cell is commercially available today and has an operating temperature between 150°C and 220°C. One of the main advantages to this type of fuel cell is the nearly 85 % cogeneration efficiency. It can also make use of impure hydrogen as a fuel but is not as efficient as the PEMFC. If gasoline is used, the sulphur must be removed (Basu, 2007:6).

- **Molten Carbonate Fuel Cell (MCFC)** - Molten carbonate fuel cells use an electrolyte composed of a molten carbonate salt mixture suspended in a porous, chemically inert matrix. They operate at high temperatures between 600°C and 700°C and require CO_2 and oxygen to be delivered to the cathode. To date, MCFCs have been operated on hydrogen, carbon monoxide, natural gas, propane, landfill gas, marine diesel, and simulated coal gasification products (Basu, 2007:6).

- **Regenerative Fuel Cell (RFC)** - As mentioned above the PEMFC uses hydrogen and oxygen to generate power (Figure 1a). The **reverse** is also true - hydrogen and oxygen can be produced by supplying water, electricity and heat to a FC (Figure 1b). This type of FC is called a Regenerative PEMFC (RFC) (Rabih, Rallieres, Turpin & Astier, 2006).

1.2 Regenerative fuel cells

When the RFC is in its normal mode hydrogen and oxygen can be produced by introducing water to the anode electrode chamber, and applying a potential across the anode and cathode. This will cause the decomposition of the water to produce oxygen at the anode side and hydrogen at the cathode side. The chemical reaction taking place in the RFC in its normal mode is called an endothermic reaction. An endothermic reaction absorbs energy to take place, in this case heat and electricity from the power source (Rabih *et al.*, 2006). The RFC in its normal mode (electrolyser mode) is shown in Figure 1b with its chemical equation. The RFC that can also be used in its reverse mode to generate power is shown in Figure 1a.

1.3 Problem statement

In order to efficiently produce hydrogen with a RFC certain parameters need to be controlled and optimised to increase the efficiency of the process. These parameters include supply voltage, water flow and temperature of the RFC.

1.4 Justification for the research: The imperatives

- Climate change owing to greenhouse gases (Farmers, 2011);

- The carbon footprint of South Africa is very high and is increasing (Laburn, 2010);
- S.A. supplier of electricity(Eskom) does not have enough power (Calldo, 2008);
- South Africa is responsible for more than 30 % of the greenhouse gases in Africa (Farmers, 2011);
- In South Africa rural areas are inhabited by over 19 million (or 39 %) South Africans who live mostly without electricity and who are very poor (Calldo, 2008).

With approximately 60 % of the population not having access to electricity, the Department of Minerals and Energy (DME) is determined to promote non-grid power as the technological equal of grid electrification (van Tonder and Pienaar, 2010).

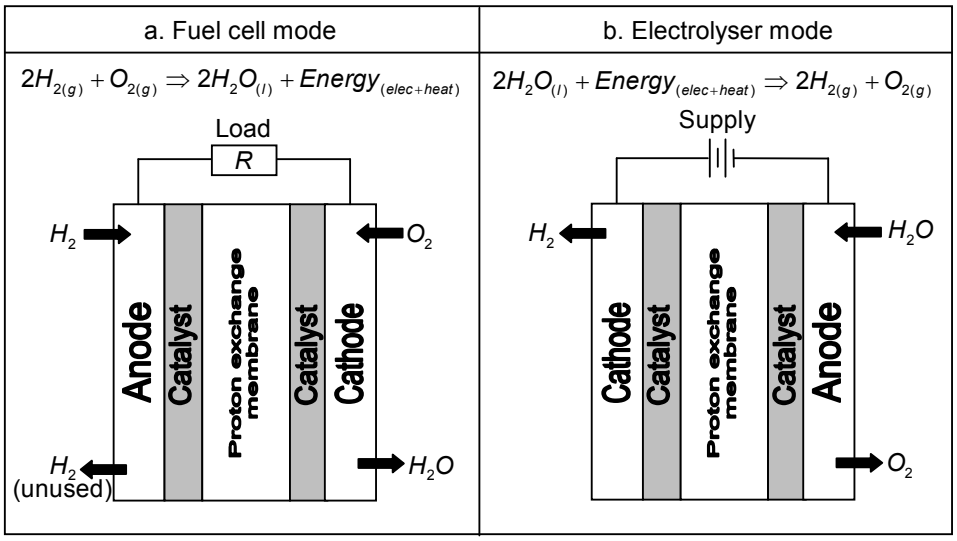

Figure 1 a RFC in fuel cell mode and electrolyser mode

By 2012, an estimated two to three million households will still have no connection to the grid (Wentzel, 2004). That means that the total number of households with no grid connection will remain almost as high as presently, however the share of grid - connected households on the total number of households will still increase constantly. As a possible solution to this problem to generate electricity small solar hydrogen systems (SHS) can be used.

Figure 2 shows a block diagram of such a SHS. Pure water and electricity from solar power sources is supplied to a RFC. In turn the RFC will produce hydrogen, which can be stored in a tank for later use. The stored hydrogen is then supplied to the fuel cell to produce electricity, when solar or wind power falls below a certain threshold. The water as a by-product of the fuel cell is stored in a water tank. This stored water may then be fed to the

RFC at a later stage in the production of hydrogen. This occurs when sufficient wind or solar power rises above the set threshold.

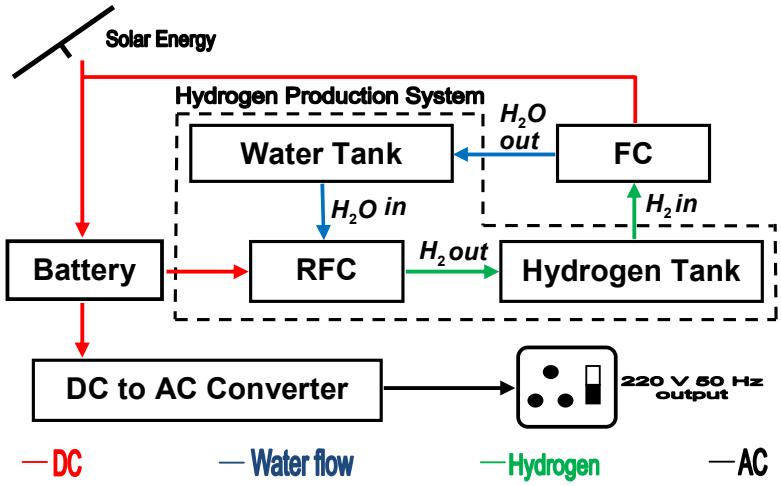

Figure 2 Solar hydrogen System

The power from the battery is connected to a DC to AC converter that will supply a 220 V 50 Hz output, which is the standard power for South Africa (Barnes & Overton, 2003). The RFC must have a high efficiency as it is powered by natural elements (wind, solar, etc.).

1.5 Aims

In order to increase the efficiency to produce hydrogen with a RFC, certain parameters need to be controlled and optimised to make the process as efficient as possible. If a RFC with a low efficiency is to be used in a sustainable energy source as seen in Figure 2 it will decrease the total efficiency of the system. The aim of this research is to increase the efficiency of the RFC by optimising the:

- Temperature of the RFC,
- Water management to the anode electrode chamber of the RFC,
- Supply voltage across the cathode and anode of the RFC,
- Pressure control of the hydrogen inside the RFC cathode chamber.

1.6 Research methodology

The optimisation of water, temperature and voltage management on a RFC will be addressed in the following manner. Firstly, an in-depth literature study will be conducted on

the operation of the RFC device. This will then be followed by the design and construction of the various components of the RFC. After all the components had been manufactured into various proprietary designs, the three cell RFC was constructed. All the necessary experiments were conducted on the three cell RFC. The results obtained from the experiments were then compared to that of the theoretical results. Finally the results were used to make certain conclusions on how to optimise the operation of the RFC taking in consideration the water, temperature and voltage management.

1.7 Delimitations

This research did not include the control of the internal pressure of the RFC. It also did not involve any construction of the physical membrane or membrane assembly components. However it did involve the construction of the RFC stack and its components.

1.8 Overview of the report

Chapter 2 – In this chapter the initial literature review and careful comprehension of the operation of a RFC is done. This study also involves the components that make up the RFC and how they are put together.

Chapter 3 - This chapter will focus on the practical design and the construction of a small three cell RFC stack and its components.

Chapter 4 - This chapter shows the experimental setup of the three cell RFC in order to perform the necessary experiments and overview of all of the experiments performed on the RFC in order to optimise its operation. The methods followed and results obtained for each experiment are also given in this chapter.

Chapter 5 - Contains conclusions obtained from the experiments conducted on the RFC and recommendations for future research.

1.9 Summary

In this chapter the background of the need to control certain aspects of the RFC to produce hydrogen efficiently, was given. The purpose of the study along with the topic of research has been given. In conclusion, an overview of the research was also represented.

Chapter 2 will give a literature review on the operation of the RFC and its components.

Chapter 2 Regenerative fuel cells (RFC)

2.1 History of the RFC

The first FC was demonstrated in 1839 by William Grove. Since the 1950s the interest in FCs grew rapidly, particularly to generate electricity for a spacecraft using safe, compact and relatively lightweight technology. In the early FCs used in the space programs, the hydrogen and oxygen were stored on board, but it was soon recognised that a reversible cell capable of both electrolysis and power generation could be the central component of a closed-loop system. The hydrogen generated could be stored for use at a later stage to generate electricity and the only input to the system would be solar energy. Early proof of the concept of a FC that can work in FC mode and RFC mode was introduced by General Electric in 1973, when a RFC with one cell showed that the reversible operation was feasible without significant deterioration of the cell membrane and catalyst (Mitlitsky, Weisberg, Carter, Dittman, Myers, Humble & Kare, 1999).

2.2 Different methods to generate hydrogen

There are a number of ways to generate hydrogen namely:

- **Steam reforming**
  Steam reforming uses thermal energy to separate hydrogen from the carbon components in methane and methanol. It also involves the reaction of these fuels with steam on catalytic surfaces. These reactions occur at temperatures between 190°C and 900°C (Grimes, Varghese & Ranjan, 2008:37-41).

- **Biological and photobiological processes**
  Biological and photobiological processes use algae and bacteria to produce hydrogen. Under specific conditions, the pigments in certain types of algae absorb solar energy. The enzyme in the cell acts as a catalyst to split the water molecules. Some bacteria are also capable of producing hydrogen, but unlike algae they require a substance to grow on (Akkerman, Jansse, Rocha & Wijffels, 2002).

- **Electrolysers with solid electrolyte (RFC)**
  Electrolysis separates the elements of water by charging it with an electrical current. The charge breaks the chemical bond between the hydrogen and the oxygen and splits the atomic components apart, creating charged particles called ions. The ions are formed at the two poles: the anode, which is positively charged, and the

cathode, which is negatively charged. Hydrogen gathers at the cathode and the anode attracts oxygen. Electrolysers with solid electrolytes are known as proton-exchange membrane (PEM) or solid-polymer electrolytes (SPE) (Grimes *et al.* 2008:18-19).

PEM technologies have resulted in electrolysers with low volume solid electrolytes and which operate at near ambient temperature that offer safe startup and shut down. The PEM electrolyser's efficiency is independent of the size of the system whilst cost increases nearly linear to size. At the moment there are two types of membranes available - du Pont's Nafion and Dow Chemical's XUS-132040.10. Both are very similar in structure. The different types of available electrolysers are listed in Table 1 (Grimes *et al.,* 2008:18-19).

Table 1. Types of electrolysers

Name	Diaphragm	Electrolyte
Conventional alkaline	Asbestos	25 - 35 % (KOH)
Advanced alkaline	Up to 90°C polymer reinforced asbestos, over 100°C poly-sulphuric and nickel net with ceramic reinforced diagram	25 - 40 % (KOH)
Polymer membrane (Regenerative Fuel Fell)	Conductive proton nafion membrane at the anode with ruthenium oxide at the cathode with platinum layer	Du Pont's Nafion membrane Dow Chemical's XUS-132040.10
Inorganic membrane	Polyatemon acidic	14 -15 % (KOH)

From the above the polymer membrane (RFC) was chosen because of the following advantages:

- They produce high purity (99.999 %) hydrogen as well as oxygen (Grigoriev, Porembsky & Fateev, 2006);
- The RFC could also work at high pressures (Grigoriev et al., 2006);
- The RFC can operate over a wide range of temperature (0 - 100°C), pressure (0 – 7000 kPa) and has a higher energy efficiency compared to the alkaline-type water electrolyser. The RFC has an energy efficiency of between 80 % and 90 % where alkaline has an energy efficiency of between 75 % and 85 % (Tsutomu and Sakaki, 2003).

2.3 Operation of a RFC

The block diagram of a typical RFC is shown in Figure 3. The operation of the RFC shown in Figure 4 is as follows: Water is introduced at the anode electrode chamber. A potential difference of more than 1.23 V is applied across the anode (positive) and cathode (negative) electrodes for the decomposition of water to take place.

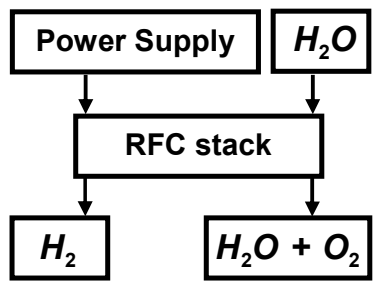

Figure 3 Block diagram of a typical RFC

At the anode a catalyst in the form of Iridium Ruthenium oxide and platinum mixture (*IrRuOx* and *Pt* black), allows the decomposition of the water molecules that forms oxygen protons (O^+) and hydrogen protons (H^+). The electron from the hydrogen atom is released into the external circuit. The O^+ does not lose its electrons but rather joins with another O^+ to form O_2 . This process corresponds to the evolution of the O_2 at the anode electrode.

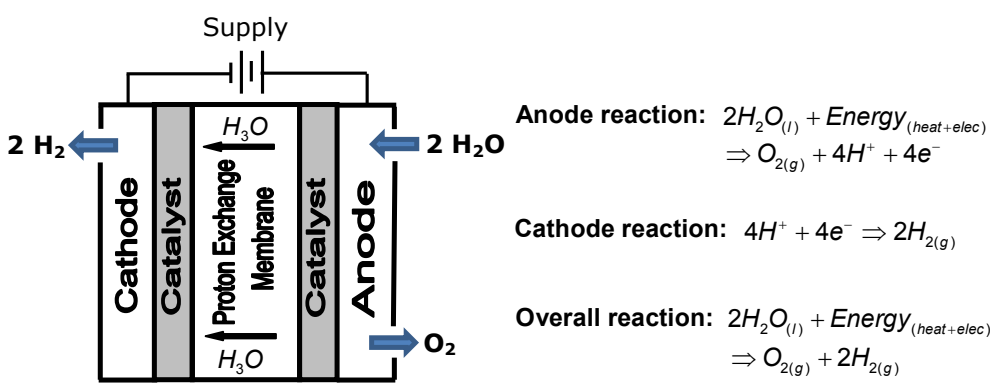

Figure 4 Operation of a RFC

The H^+ proton joins up with the H_2O in the membrane and forms hydronium ions (H_3O) that are used to transport the H^+ from the anode to the cathode under the effects of the potential that was applied across the anode and cathode. The electrons that were previously lost to

the external circuit are now re-joined with the H^+ proton at the cathode catalyst in the form of platinum black (Pt black) and forms a hydrogen (H) atom. Two of these atoms combine and form an H_2 molecule. The regenerative fuel cell produces gases at a constant rate and not in bubble fashion, which allows the cell to produce gas at a constant pressure without placing physical strain on the membrane (Swanepoel, 2005:13-14). If the supply voltage to the RFC increases the current will also increase. When the current increases the rate of the reaction will increase and will cause an increase in oxygen and hydrogen produced.

2.4 Components of the RFC

Shown in Figure 5, the RFC consists of a proton exchange membrane coated with an electrocatalyst which forms the membrane electrode assembly (MEA) that is sandwiched between two plates; the plates are called the anode and cathode flow field plates.

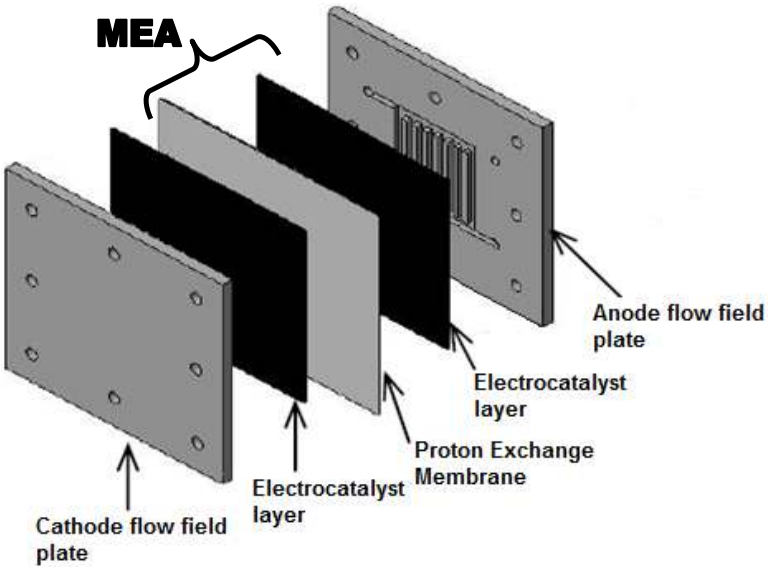

Figure 5 Basic structure of the RFC

2.4.1 MEA

The MEA is also known as the catalyst-coated membrane (CCM) and is considered the 'heart' of the PEM fuel cell device. The MEA consists of a co-polymer membrane with an anode electrode on the one side and a cathode electrode on the other. The electrodes are only a fine layer of a fine compound painted or pressed on the membrane. The electrodes are doped with a noble metals catalyst such as Pt or $PtOx$. After the electrodes are doped

with a noble catalyst it forms electrocatalysts (Ledjeff, Mahlendorf, Peinecke & Heinzel, 1994).

2.4.2 Proton exchange membrane

The functions of the proton exchange membrane are to separate the reactant gases and conduct hydrogen protons through its structures when hydrated with water molecules. Grubb and Niedrach discovered the organic-based proton exchange membranes in 1959 (Chen, 2003:2-30). Nafion is the best known ionomer membrane for the use as a solid proton conducting electrode in electrochemical technology. The Nafion membrane has a copolymer molecular architecture. The molecule is characterised by a hydrophobic polyterafluor-oethylene backbone chain and regulararly spaced shorter perfluorovinyl chains on either side, each terminated by a strongly hydrophilic sulfonate ionic group. Figure 6 shows the Nafion structure (Haubold, Vad, Jungbluth & Hiller, 2001).

The mechanical strength of the Nafion membrane arises from the interaction of the perfluorinated backbone chains. For its use as a protonic conductor the protons membrane contains about 20 wt.% water forming hydration shells around the fixed covalently bonded anionic sulfonic acid groups. The conductivity is assigned to hydrated protons (H_3O) as protonic charge carriers. For the transport through the membrane a percolated spongelike microstructure supplied the transport channels (Haubold *et al*., 2001)

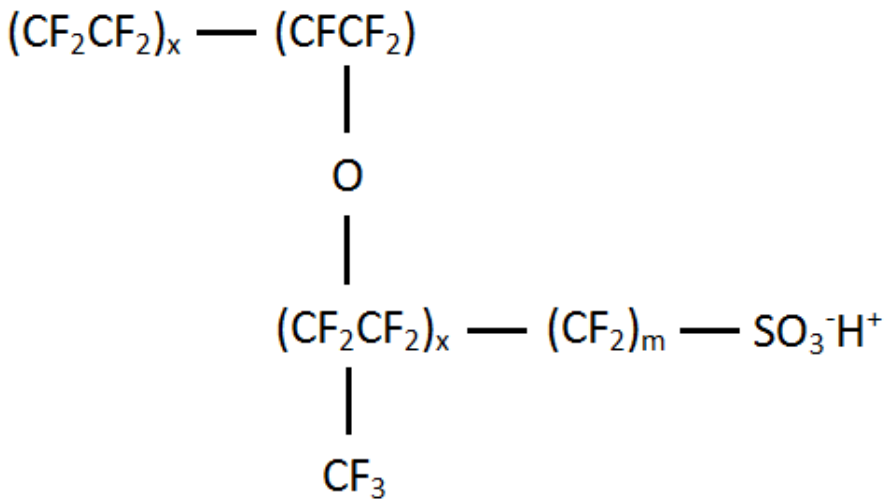

Figure 6 Nafion structure

Nafion membranes are available in 15 different versions (Ion Power, 2005). The most of the companies providing membrane setups for FCs would use one or more of these membranes

in various configurations as seen in Table 2 (Swanepoel, 2005:25).

Table 2. Various membranes and their applications

Application	Membrane type
H_2/O_2 FC	Nafion N-105
Reformate fuel/Air or H_2/Air	Nafion N-112
Direct methanol FC (DMFC)	Nafion N-117
RFC	Nafion N-105 or Nafion N-115
RFC in FC mode	Nafion N-115

It has been found that the membrane used for a DMFC in most instances was the Nafion N-117 with a thickness of 183 µm. This is a considerable distance for the protons to travel across in the conductive phase and will increase the resistance and the strength of the membrane. If a thinner membrane is used (e.g. Nafion N-105) the internal resistance as well as the strength of the membrane, will decrease (Swanepoel, 2005:25). The thicknesses of the different types of Nafion membranes are shown in Table 3.

Table 3. Nafion membrane thickness

Membrane type	Thickness (µm)
N-112	51
N-1135	89
N-115 & N-105	127
N-117	183
NE-1110	254

According to Lynntech Industries the choice of membrane to be used in a RFC is the Nafion N-115 membrane because of its thickness. It has a typically thickness of 127 µm, the reduced thickness of the membrane allows for a balance between the internal resistance and the strength of the membrane. Owing to the thickness of the N-115 membrane it can operate at high pressures (0 – 7000 kPa) (Smith, 2000).

2.4.3 Electrocatalyst

The electrocatalyst is a material that accelerates a chemical reaction but is not consumed in the process. The elecrocatalyst layers play a critical role in defining the performance of the

MEA. Without them, the MEA would not function. To play its essential role, an electrocatalyst has to fulfil several requirements (Thompsett, 2003:139):

- It needs to provide high intrinsic activities for the electrochemical oxidation of a fuel cell at the anode and for the reduction of dioxygen at the cathode,
- Good durability because PEMFCs are expected to operate for long periods,
- Good electrical conductivity to minimize resistive losses,
- Inexpensive to fabricate to reduce the cost of the MEA.

The development of electrocatalysts for state-of-the-art PEMFCs has relied heavily on concepts and formulations developed for earlier fuel cell technology. As with any heterogeneous catalyst material, a number of fundamental requirements are necessary for good performance (Thompsett, 2003:140):

- High intrinsic activity,
- Maximum number of these sites,
- Electrical conductivity,
- Good interaction with ionomer,
- Reactant gas access,
- Stability in contact with reactants, products, and electrolytes.

Research over several decades has found that platinum and platinum-containing catalysts are the most effective catalyst materials, in terms of both activity and stability (Hoogers, 2003:121). In the RFC *Pt* black is used as a catalyst at the hydrogen side or alternatively at the cathode. However the cathode catalyst must be able to retain its physical integrity and resist corrosion in the presence of water molecules dragged across from the anode side by protons during RFC mode (Doddathimmaiah, 2006:43-47).

The anode catalyst (oxygen side) is typically more difficult and challenging to design and construct, because of the difficulty in finding a catalyst material that functions equally well in both RFC and FC mode. *Pt* black in the anode catalyst performs well in the FC mode but poorly in the RFC mode. Thus the mixture of catalyst materials is usually employed on the anode side. *Pt* black is commonly retained in the mixture for the FC mode functionality, while a range of noble metals and their oxides have been investigated as the additive to play the lead role in the RFC mode. Since the water is introduced at the anode chamber during the RFC mode the catalyst must be able to retain its structure and functionality in the presence of water. Materials that can be mixed with *Pt* black for the anode catalyst include

pure metals (iridium (*Ir*), ruthenium (*Ru*) and rhodium (*Rh*)) or oxides such as iridium oxide (*IrOx*) and ruthenium oxide (*RuOx*) (Doddathimmaiah, 2008:43-47).

It has been found that in a mixed *IrPt* black catalyst the *Ir* will be the dominant conductor to the oxygen-evolution reaction in the RFC mode, but will be practically inactive in the FC mode when the *Pt* will be active. *RuOx* plays a similar role and is mixed with *Ir* since the latter is less costly and also has better electrical conductivity. The advantages of using the oxides rather than pure metals are lower cost and that they have a greater resistance to corrosion (Doddathimmaiah, 2008:43-47). The catalyst loadings are loaded in such a way to achieve the best performance vs. cost. If the catalyst loadings are increased, the increase in performance will not justify the increase of the cost. The best catalyst loadings on the Nafion N-115 membrane according to Lynntech are:

- Anode: 20 µg/mm^2 *IrRuOx* and 20 µg/mm^2 *Pt* Black
- Cathode: 20 µg/mm^2 *Pt* Black

2.4.4 Bipolar Plates

The MEA of the RFC is sandwiched between two plates, that are called the anode and cathode flow field plates. Flow channels are conveniently machined into the plates to allow fuel distribution. The one side of the flow field plate serves as the cathode and the other side serves as the anode to the adjacent cell plate that is called a bipolar plate as demonstrated in Figure 7 (Dihrab, Sopian & Zaharim, 2008).

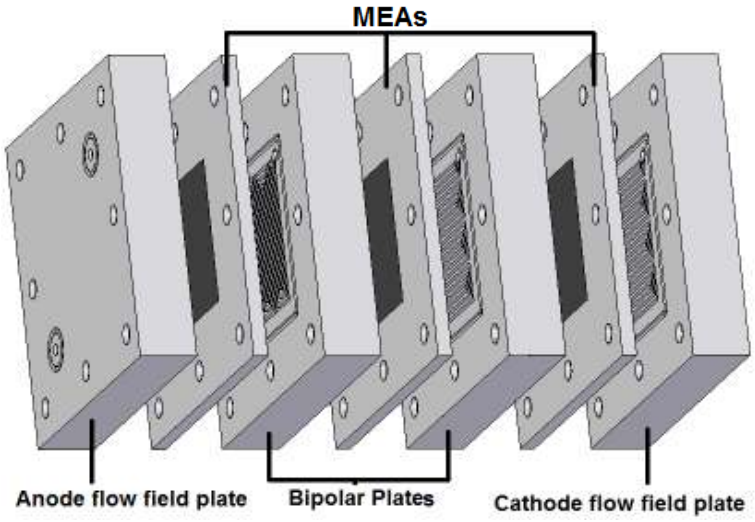

Figure 7 Bipolar Plates

Bipolar plates are known to have six functions (Dihrab *et al*., 2008):

- Distribute the fuel and its oxidants within the cell,
- Facilitate water management within the cell,
- Separate individual cells in the stack,
- Transport currents away from the cell,
- Facilitate heat management,
- Even thermal distribution.

Bipolar plates can be made out of a number of materials such as: Graphite, metals, carbon composites and carbon composites polymer (Oh, Yoon & Park, 2004).

2.4.4.1 Plate materials

According to Heinzel *et al*. (2009) the requirements of a material used for a bipolar plate are as follows:

- Good electrical conductivity (>10 S/mm),
- High thermal conductivity (>2 W/mm),
- High chemical and corrosion resistance,
- Mechanical stability towards completion forces,
- Low permeability for hydrogen,
- Low cost,
- Low weight and volume.

Two types of bipolar plates were investigated in this research namely metallic bipolar plates and graphite bipolar plates:

A. Metallic bipolar plates materials

The first applications of the PEMFCs were very costly. Here, expensive corrosion-resistant materials were used as bipolar plates. Even for stainless steels the cost factor is high, therefore substrates and coatings have been investigated in order to find the optimal material combinations. If the metal used for the bipolar plates releases metal ions the membrane can be contaminated and will reduce the activity of the electrode catalyst. Bipolar plates made of aluminum, stainless steel and titanium have been subject to different types of coatings to improve their corrosion resistance. The coatings can be distinguished between two types (Heinzel *et al.*, 2009).

- Carbon-based coating - The coatings mainly comprise conducting polymers e.g. diamond-like carbon, poly-pyrrole and polyaniline (Heinzel, 2009).
- Metal-based coatings - The coatings include noble metals, metal nitrides and early transition metal elements such as molybdenum, vanadium and niobium that form a thin oxide layer that passivates the underlying metal against corrosion (Heinzel, 2009).

Coated metals for bipolar plates seemed to have achieved the corrosion stability but only for a relatively short operational life.

B. Graphite bipolar plates materials

The word graphite is derived from the Greek word 'grapho'. Graphite is one of four forms of crystalline carbon; the others are carbon nanotubes, diamonds and fullerenes. Graphite occurs naturally in metamorphic rocks, such as geneiss, marble and schist. Graphite is flexible but not elastic. Graphite also has a melting point of 3927°C and is highly refractory. Graphite has both metallic and non-metallic properties which makes it suitable for many industrial applications. The metallic properties include electrical and thermal conductivity. The non-metallic properties include high-thermal resistance, inertness, and lubricity. The combination of conductivity and high thermal stability allows graphite to be used in many applications such as batteries, refractories and fuel cells however, machining of the flow channels into the graphite plates is a complicated and time consuming process that results in high cost (Olson, 2003).

More over graphite plates are brittle and porous; they have to be coated or be of very high quality to be impermeable to the hydrogen (Heinzel, 2009). Another promising candidate as the bipolar plate is graphite foil. It is obtained from high-purity natural graphite flakes, which are processed into a continuous foil by acid and thermal treatment to process without any resins or binders. The graphite foil shows good electrical conductivity and high chemical resistance but in order to be used in a bipolar plate it must be treated with a resin. An important characteristic of graphite foil is its compressibility. Flow fields are incorporated into the foil by embossing (Heinzel, 2009). Embossing is a process for producing raised or sunken designs or relief in the graphite foil. This process can be made by means of matched male and female roller dies, or by passing the graphite foil between rolls of the desired pattern.

For stationary PEMFC applications, bipolar plates are the only alternative, showing good long-term stability and will not contaminate the membrane. The graphite bipolar plate is significant cheaper than the coated metal bipolar plates and offers the same performance

but is much heavier than the metal plate thus if graphite is to be used as a bipolar plate it will account for 80 % of the stack's weight (Heinzel, 2009).

Graphite plates have very high bulk conductivity ($1.27x10^4$ S/mm), greater than the 10 S/mm stated by Heinzel *et al*. (2009). The mass distribution of a 33 kW PEMFC employing graphite bipolar plates versus metallic bipolar plates that are electroplated with a noble metal are shown in Figure 8 (Li and Sabir, 2005). The graphite is generally heavier than the coated metal plates but has a much higher conductivity and better overall performance.

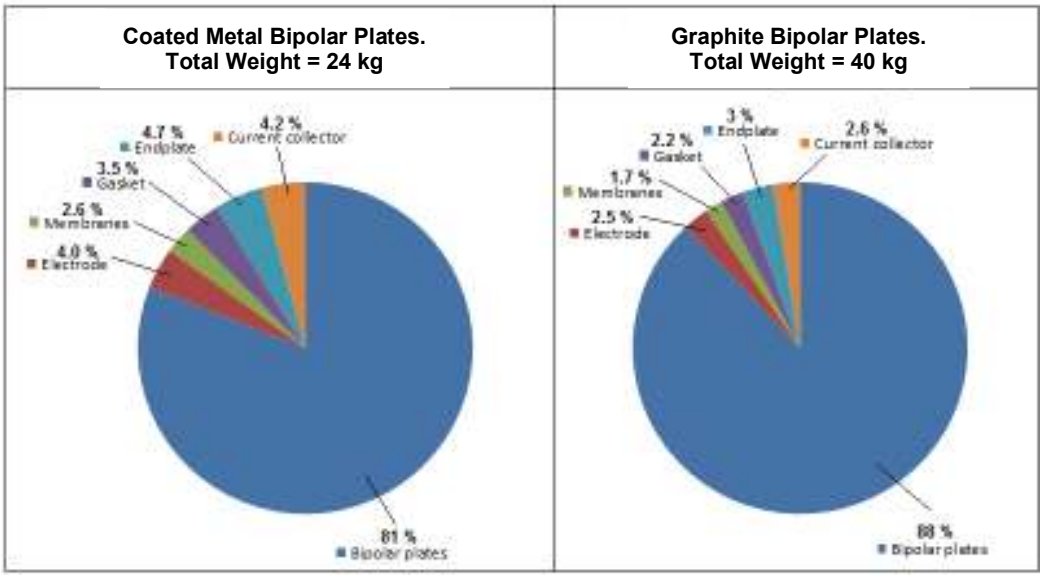

Figure 8 Mass distribution in a 33kW PEMFC stack (Li and Sabir 2005:5).

2.4.4.2 Flow field designs

The distribution of reactance over the membrane is critical to the operation of the RFC. According to Li and Sabir (2005) the appropriate distribution of reactance over the membrane can increase the power output density of a cell or stack up to 50 %. According to Hoogers (2003: 106) a balance must exist between the supply of reactance and the current conduction of the bipolar plate design. The best conductor would be a solid blank sheet, which affords low contact resistance and also allows no gas access to the MEA. An entire open structure would allow the full access of reactance to the MEA, but will have a high contact resistance allowing no current to flow. Flow field designs employed by commercial FC stack developers are well-kept secrets, but on the academic side certain authors proposed a number of flow fields. The most effective, popular and reliable of these designs for a RFC are discussed below (Swanepoel, 2005:50-54).

A. Pin type

This flow field consists of a number of pins arranged in a regular pattern; these pins can be in any shape or size, although cubical and circular pins are often used in practice. Pin-design flow fields result in low reactant pressure drops. However reactance flowing through the pin type bipolar plate tends to follow the path of least resistance across the flow fields, which may lead to channeling and formation of stagnant areas. Uneven reactant distribution therefore results in poor water removal and poor FC performance (Li and Sabir, 2005). An example of a pin type flow field is shown in Figure 9.

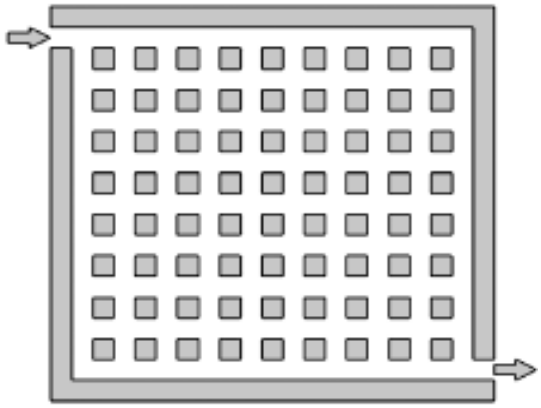

Figure 9 Pin type

B. Straight and parallel channel type

Parallel channels are used to connect straight flow fields shown in Figure 10. The problem with this type of flow field is that water forms (cathode electrode) in the areas where the reactant flow rate is the least in the FC mode, causing water buildup. When water buildup occurs it will result in low and unstable voltages generated by the FC. The pressure drop between the inlet and the outlet is low, resulting in the cells further on in the stack not receiving enough reactant flow rate. This leads to cells being starved of effective reactance (Kordesch & Simader, 1996:4-19).

C. Serpentine channel type

This flow field resolves most of the problems addressed in the pin type and straight and parallel channel type. The reactance only follows one path from the inlet to the outlet (see Figures 11 and 12). This method increases the distribution flow pressure across the cell or stack. Although the pressure drop between the inlet and the outlet prevents water from building up in the channels, it does result in an increase in concentration gradients. Many single or short stacks (less than 10 cells) use single continuous serpentine flow topology.

These designs suffer from the removal of water under high current densities (>5 $mA.mm^{-2}$) (Swanepoel, 2005:50-54).

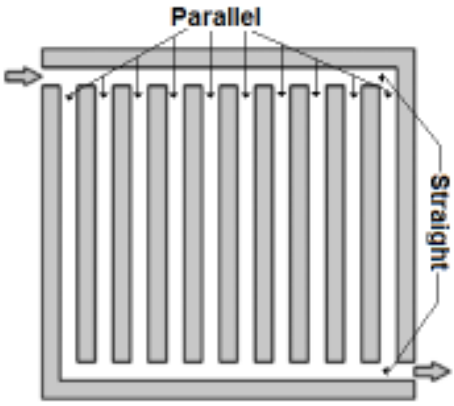

Figure 10 Straight and parallel channel type

In order to combat this problem several continuous serpentine flow fields are used (Figure 12). This design has an added benefit of a limited pressure drop between the inlet and the outlet, decreasing the concentration over voltages and number of stagnant areas (Swanepoel, 2005: 50-54). The several continuous serpentine flow field platform has been found to increase the overall power of a stack by up to 50 %. The continuous serpentine flow field is very popular among FC designers. Mennola's (2007) research showed that the following design considerations delivered the best results for continuous serpentine flow fields:

- Channel width is preferred between 1.14 and 1.4 mm,
- Channel depth must be kept between 1.02 and 2.04 mm,
- Land widths should be between 0.89 and 1.4 mm.

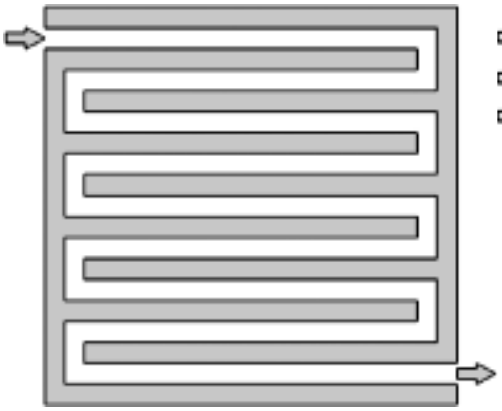

Figure 11
Single continuous serpentine

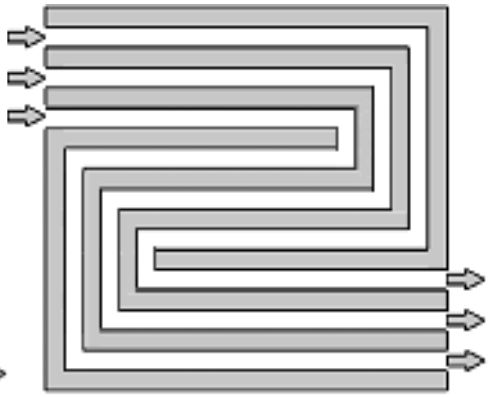

Figure 12
Several continuous serpentine

D. Integrated channel type

In Figure 13 the integrated flow field is shown. One of the functions of the bipolar plate is to ensure even thermal distribution and thermal management across the entire stack. The integrated topology has been devised to aid the bipolar plate in this task.

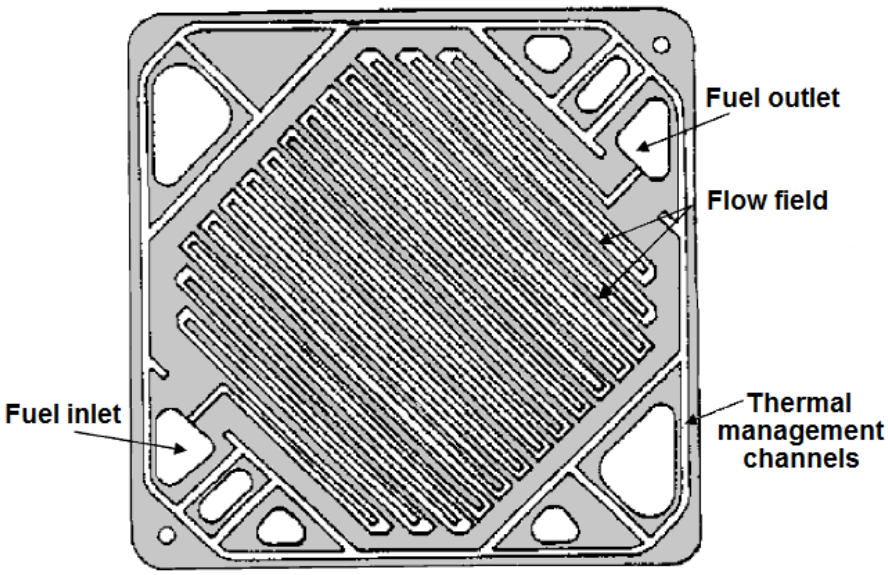

Figure 13 Integrated channel flow type

The integrated channel type consists of any flow topology with extra thermal distribution and thermal management channels. The thermal channels can be used to warm up the cell (flow of warm liquid) or to cool down the cell (flow of coolant). This topology eliminates the need for the use of extra cooling plates in the stack (Li and Sabir, 2005).

2.5 Chemical thermodynamics

The operation of a RFC revolves around the chemical reaction taking place within the cell. The reactions of the RFC in its FC and RFC mode are:

$$H_2O + Energy_{(Electric+heat)} \Leftrightarrow H_2 + \frac{1}{2}O_{2(g)} \quad (1)$$

Accordingly Gibbs energy or Gibbs function is the chemical potential that is minimised when a system reaches equilibrium at constant pressure and temperature. It is derived with respect to the reaction coordinate of the system that vanishes at the equilibrium point. As

such, it is a convenient criterion of spontaneity for presses with constant pressure and temperature. The Gibbs energy equation follows (Lee, 2001):

$$\Delta G = \Delta G^o + RT \ln \frac{P_M^m P_N^n}{P_A^a P_B^b} \tag{2}$$

Where:

$\Delta G^o \equiv$ Gibbs standard free energy ($kJ.mol^{-1}$)

$R \equiv$ Universal gas constant (8.314 $J.mol.K^{-1}$)

$T \equiv$ Absolute temperature in Kelvin (K)

$P_M^m P_N^n \equiv$ Pressure of reactants in kPa

$P_A^a P_B^b \equiv$ Pressure of products in kPa

The enthalpy (ΔH) is the preferred expression of system energy changes in many chemical, biological, and physical measurements, because it simplifies certain descriptions of energy transfer. This is because a change in enthalpy takes account of energy transferred to the environment through the expansion of the system under study. The total H of a system cannot be measured directly. Thus, a change in enthalpy, ΔH , is a more useful quantity than its absolute value. The change ΔH is positive in endothermic reactions, and negative in exothermic processes. ΔH of a system is equal to the sum of non-mechanical work done on it and the heat supplied to it (Lee, 2001). The theoretical energy required for the reaction to proceed, can be expressed through the following equation:

$$\Delta H = \Delta G + T\Delta S \tag{3}$$

Where:

$\Delta H \equiv$ Enthalpy change of reaction

$\Delta S \equiv$ Entropy change

Standard temperature and pressure (STP) are standard sets of conditions for experimental measurements, to allow comparisons to be made between different sets of data. Under STP, the enthalpy change of reaction based on liquid water is ΔH = 285.8 kJ/mol. The corresponding change in Gibbs free energy at STP is ΔG = 237.2 kJ/mol (Larminie and Dicks, 2003:31-33). In other words 237.2 out of 285.8 kJ/mol, or 83 % of the minimum energy required to electrolyse liquid water under standard conditions must come from electricity. The other 17 % could theoretically by supplied by heat or by electricity as well. International Standard Metric Conditions for natural gas and similar fluids is 273.15 K and

100 kPa (Doddathimmaiah, 2008: 29). Two distinct cell voltages can be calculated from the change in Gibbs free energy ΔG and the reaction enthalpy ΔH . The first one is called the reversible voltage (E^o).

$$E^o = \frac{-\Delta G}{2F} \tag{4}$$

The second one is called the thermoneutral cell voltage (E^{tn}).

$$E^{tn} = \frac{-\Delta H}{2F} \tag{5}$$

The minimum voltage necessary for the RFC electrolysis process is E^o . If the supply voltage to the RFC is above E^{tn} the process becomes exothermic, meaning that the heat is generated inside the RFC and all the energy required comes from electricity. When the RFC is operated between E^o and E^{tn} the process is endothermic and part of the energy required for the electrolysis operation comes from heat (Doddathimmaiah, 2008: 28-31). The E^o and E^{tn} of the RFC will be calculated at STP and the values of ΔG and ΔH are found on the list of thermodynamic properties of various substances (obtainable in Annexure A).

$$\begin{aligned} E^o &= \frac{-\Delta G}{2F} \\ E^o &= \frac{-(237200)}{2(96485)} \\ E^o &= 1.229 \text{ V} \end{aligned} \tag{6}$$

$$\begin{aligned} E^{tn} &= \frac{-\Delta H}{2F} \\ E^{tn} &= \frac{-(-285830)}{2(96485)} \\ E^{tn} &= 1.48 \text{ V} \end{aligned} \tag{7}$$

At higher temperatures of 100ºC the water has a lower free energy value because steam will form, as mentioned before, if the temperature changes the Gibbs free energy will also change. This following calculation will prove that if the temperature increases the required potential for the electrolysis process will decrease (compared to equation 6):

$$E^o = \frac{-\Delta G}{2F}$$

$$E^o = \frac{-(228200)}{2(96485)} \qquad (8)$$

$$E^o = 1.183\ V$$

The voltage at which the RFC requires for the decomposition of water is theoretical 1.229 V (seen in equation 6) but there are a number of over-voltages active on each of the electrodes. This will influence the voltage value because it will oppose the current flow or prevent the reactants/products from reaching the active catalyst sites. The voltage necessary for the decomposing of water for the RFC is increased to a much higher value of 1.5 V where gas molecules were first produced (Swanepoel, 2005:74-77).

2.6 The HOGEN GC hydrogen generator

The HOGEN GC hydrogen generator uses AC electric power and deionized water to produce a continuous stream of pressurized scientific grade (99.9999 %) hydrogen gas and automatically maintains a user-selected downstream pressure. The hydrogen is produced via a PEM RFC stack. The HOGEN GC hydrogen generator, available in either 300 or 600 cc/min hydrogen production capabilities, is suitable for use in laboratories and light industrial environments. HOGEN GC systems are replacing cylinders today in applications where an ultra-high pure, medium pressure, electrolytic hydrogen gas supply makes processes safer, easier, more productive and more accurate. Figure 14 shows the side view of the HOGEN GC hydrogen generator.

Figure 14 HOGEN GC hydrogen generator

Figure 15 shows a block diagram of the HOGEN GC generator and work as follows: The water is supplied to the RFC by means of a water pump and a power supply supplies a fixed voltage to the RFC. The hydrogen that is produced by the RFC is fed to the water trap; this is done to remove the water from the water hydrogen mixture. The water trap will drain the water if it reaches a certain level within the water trap. Before the produced hydrogen is released to the external supply output the purity is tested to determine if the gas purity is 99.9999 %. The purity of the gas is tested by means of the Thermal Conductivity Detector (TCD). If the purity is less than 99.9999 % the produced hydrogen will not be released to the external supply output but will be vented and the system will shut down. The water trap also serves as a hydrogen buffer tank to ensure a more stable hydrogen output.

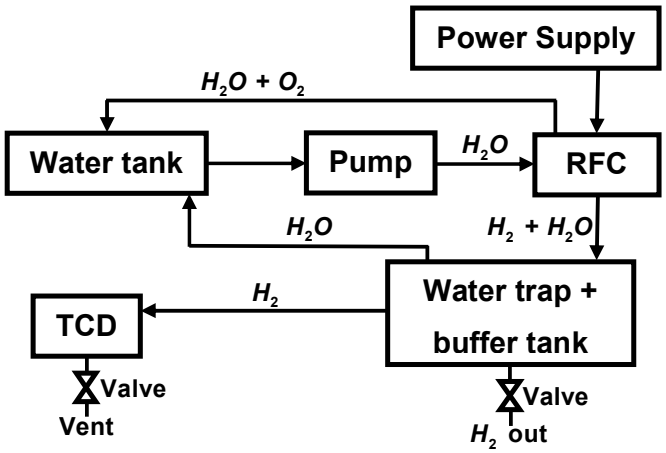

Figure 15 HOGEN GC block diagram

2.7 Water

The water used for the RFC must be distilled water; distilled water is pure H_2O with no impurities. If the water used contains any impurities it will reduce activity of the electrode catalyst which means the destruction of the RFC. Another major problem is the H_2 and O_2 produced will contain impurities and will not be 99.9999 % pure. The elements that are most harmful to the electrode catalyst are CO and CO_2. A MEA with a mixture of Pt and Ru is proposed as having the best tolerance to CO and CO_2 poisoning (Thompsett, 2003:5-6).

According to Thompsett (2003:5-6) in the FC mode it is well known that CO bonds strongly to the Pt particle sites thus reducing the sites available for the H_2 adsorption which means a decrease in performance. The CO_2 poisoning is in a lesser degree than CO; CO_2 at levels

around 25 % of the fuel volume supplied to the FC affects the performance and operation because the Pt sights are poisoned with CO molecules that are produced through the reverse water-gas shift reaction seen below:

$$H_2 + CO_2 \rightarrow H_2O + CO$$
$$CO_2 + 2Pt - H \rightarrow Pt - CO + H_2O + Pt \tag{9}$$

2.8 Effect of temperature on the RFC

The temperature at which the redox reaction takes place producing H_2 has an effect on the rate of the reaction. Higher temperatures will increase the rate at which the reaction takes place but are only effective up to 100°C. Below freezing point the reaction will not take place any more owing to the fact that the water molecules inside the membrane freezes and no proton conduction can take place (Swanepoel, 2005:14). In the thesis of Aksakal (2007:49-50) it was observed that the increase in temperature of the RFC decreased the potential difference. The RFC was tested at 30°C, 40°C and 50°C; the RFC could not be tested at higher temperatures owing to clogging by melted silicon gaskets. Figure 16 shows the results obtained by Aksakal (2007:49-50).

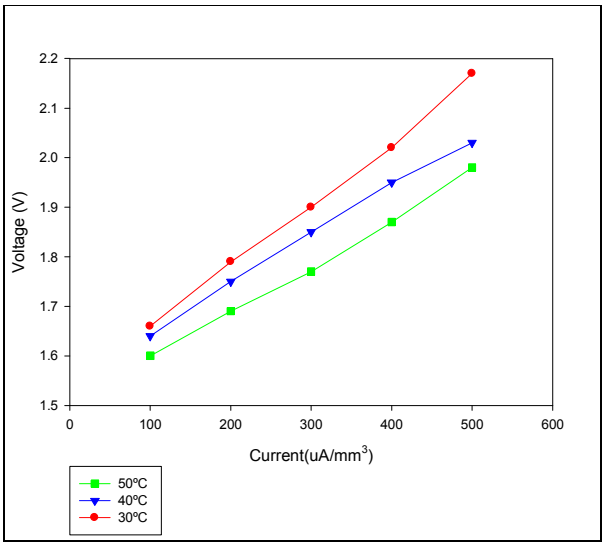

Figure 16 Effects of temperature on the RFC

2.9 Summary

This chapter considered the different methods of producing hydrogen. The history, theory and the operation of the RFC were discussed. The different components that make up the

RFC were also noted; the components included Membrane Electrode Assembly (MEA), Proton Exchange Membrane (PEM), electrocatalyst, different types of bipolar plate materials and their flow field designs. The operation of the HOGEN GC hydrogen generator was studied and explained. The reversible and thermo-neutral cell voltage of the RFC were calculated to determine the operation voltages. The effect that the temperature has on the operation of the RFC as well as the cause to membrane poisoning was given.

In Chapter 3, the physical design of the three cell RFC will be shown with regards to the theoretical study addressed in Chapter 2.

Chapter 3 Design of a Regenerative Fuel Cell

3.1 Introduction

The previous chapter considered the theory and operation of the RFC. The underlying theory regarding the modelling of a RFC stack was also discussed. This chapter will focus on the practical design and the construction of a small three cell RFC stack and its components as shown in Figure 17.

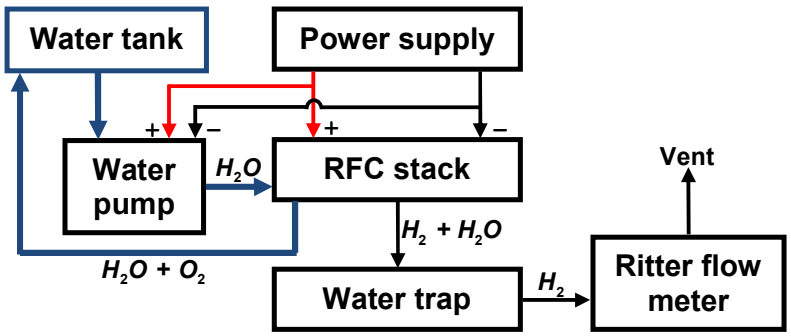

Figure 17 RFC block diagram

For the research a three cell RFC stack was chosen because if a smaller stack were used the Ritter flow meter would not be able to measure the flow of H_2 at low voltages. But if a bigger stack were used the current drawn by the stack gets too high under high voltages namely 2 V per cell.

3.2 Bipolar plates

As shown in the previous chapter graphite bipolar plates meet the requirements for the material to be used as bipolar plates. Graphite was chosen because of:

- Excellent chemical resistance,
- Good thermal conductivity,
- High bulk conductivity (1.27×10^4 S/mm), greater than the required 10 S/mm,
- Showing good long-term stability and will not contaminate the membrane,
- The graphite bipolar plate is significantly cheaper than the coated metal bipolar plates and offers the same performance but is heavier than coated metal bipolar plates.

In order to select the best flow field topology for the RFC, several factors were taken into consideration (Swanepoel, 2005:50-54):

- Flow fields designs must allow the reactant to be in the liquid and gaseous form, especially at the O_2 electrode;
- Distribution of the reactants needs to be as even as possible;
- Effective water removal when the RFC is switched from RFC mode to FC mode.

The different topologies with their disadvantages are shown in Table 4. The flow topology must be suitable for both the FC mode and the RFC mode, because the RFC can work in both modes. The three continuous serpentine type flow field topology was chosen because it resolved the disadvantages of the pin type, straight and parallel type and single continuous serpentine type as seen in Table 4.

Table 4. Flow topologies

Flow field topology	Disadvantage
Pin type	Uneven reactant distribution and poor water removal
Straight and parallel type	Poor water removal and low pressure drop between inlet and outlet
Single continuous serpentine type	These designs suffer from the removal of water under high current densities (>50 $\mu A/mm^2$)
Three continuous serpentine type	None (all the problems mentioned above are addressed in this topology

In Chapter 2 Mennola (2007) stated that the width of the channels showed the best results if it were between 1.14 mm and 1.4 mm. A channel width of 1.2 mm was chosen since this was the smallest width that the milling machine could produce. The research also showed that the land width had the best results if it were between 0.89 mm and 1.4 mm. To keep a 50 % balance between the flow of reactance and conductivity a land width of 1.2 mm was chosen (the same as the channel width). Lastly the research showed that the channel depth had the best results if it were between 1.02 mm and 2.04 mm; a channel depth of 1.5 mm was chosen.The dimensions of the graphite bipolar plate were 105 mm x 105 mm; this was the smallest size that would still allow adequate sealing of the stack. The thickness of the

bipolar plate was chosen to be 20 mm. If the thickness is reduced it becomes difficult to handle and machine because graphite is very brittle.

It was decided to use O-rings to seal the RFC between the MEA and the bipolar plate because it was observed in previous studies sealing the fuel cell with rubber gaskets proved to be unsuccessful and leaked hydrogen. The smallest O-ring cord was used which had a diameter of 1.5 mm. The O-ring groove has a width of 2 mm and a depth of 1 mm. The O-ring groove is 5 mm away from flow channels as can be seen in Figures 18 to 20. On the end plate side the O-ring with an inner diameter of 11 mm and an outer diameter of 15 mm was used to seal the endplate and the anode and cathode flow field plate. The O-ring groove has a diameter of 15 mm on the outside and 11 mm on the inside with a depth of 1.4 mm.

The RFC consisted out of an anode flow field plate, cathode flow field plate and two middle bipolar plates. In the anode and cathode flow field plate a small pipe is linked to the main inlet and outlet holes shown in Figure 18 and 19. This was done to supply the middle bipolar plates with H_2O as well to connect all the H_2O and O_2 outlets together. All the H_2 outputs are also connected together to one output which will be at the cathode flow field plate. The middle bipolar plate has four small pipes each of them is connected to an H_2O in or out hole or an H_2 out hole. The bipolar plate designs can be seen in Figure 18 to 20.

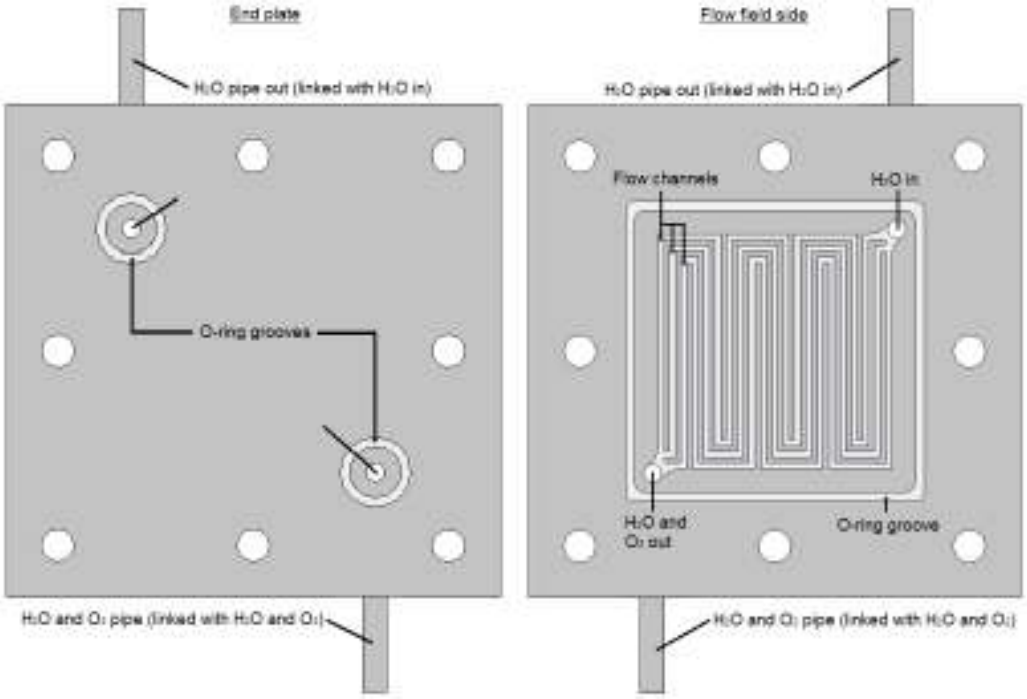

Figure 18 Anode flow field plate

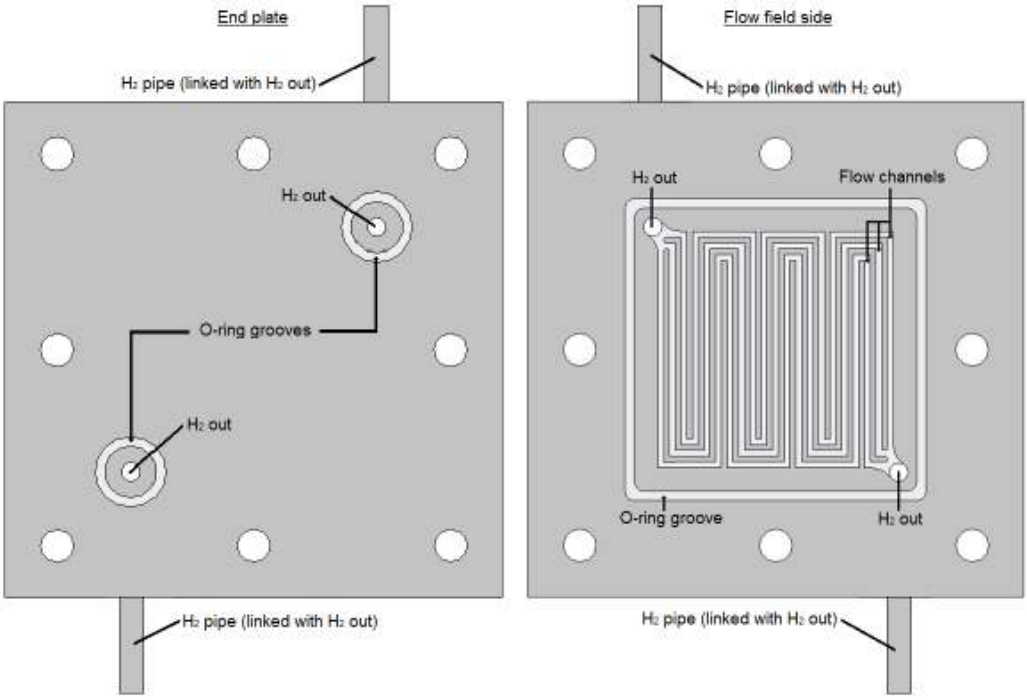

Figure 19 Cathode flow field plate

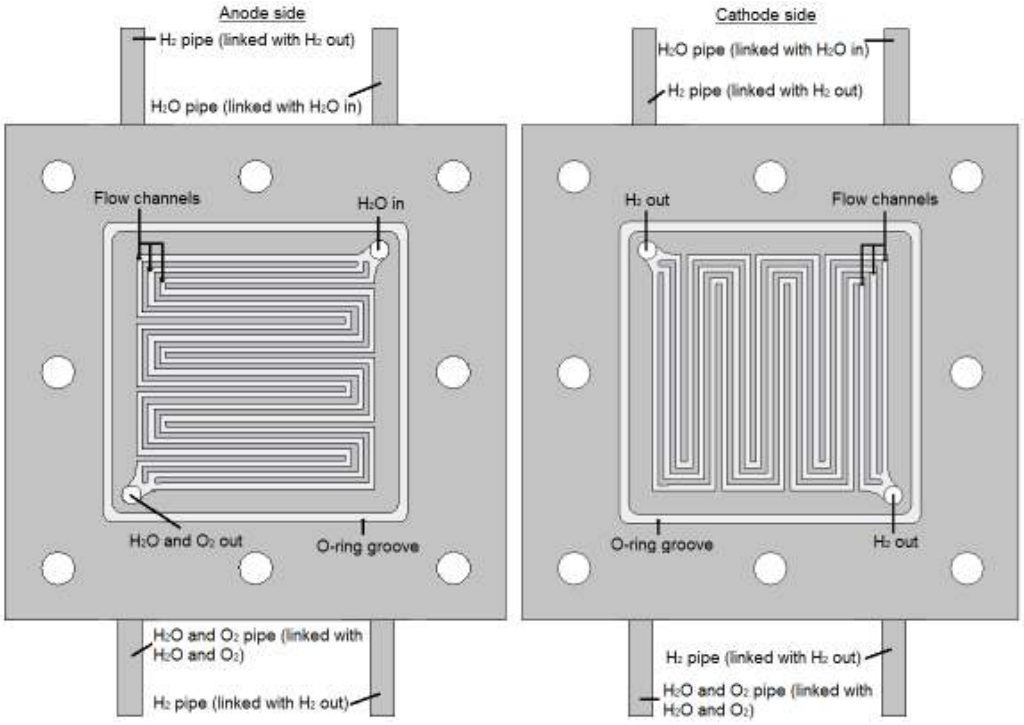

Figure 20 Middle bipolar plate

3.3 MEA

A Nafion N-115 MEA was chosen for the construction of the RFC because according to Lyntech this is the best MEA for water electrolysis addressed in Chapter 2. The MEA has an active area of 50 mm x 50 mm and was mounted on a supporting frame with an area of 100 mm x 100 mm. The active area has electrocatalyst loadings of 20 μg/mm^2 *IrRuOx* and 20 μg/mm^2 *Pt* Black on the anode and 20 μg/mm^2 *Pt* Black on the cathode. The Nafion N-115 MEA is seen in Figure 21.

Figure 21 Nafion 115 MEA

3.4 Final stack assembly

The exploded view of the RFC is shown in Figure 22. At each end of the stack is an aluminum end plate which is used to ensure adequate and uniform contact pressure between the bipolar plates and the MEAs. The entire stack assembly is compressed together using eight bolts. The photograph of the complete three cell RFC is shown in Figure 23.

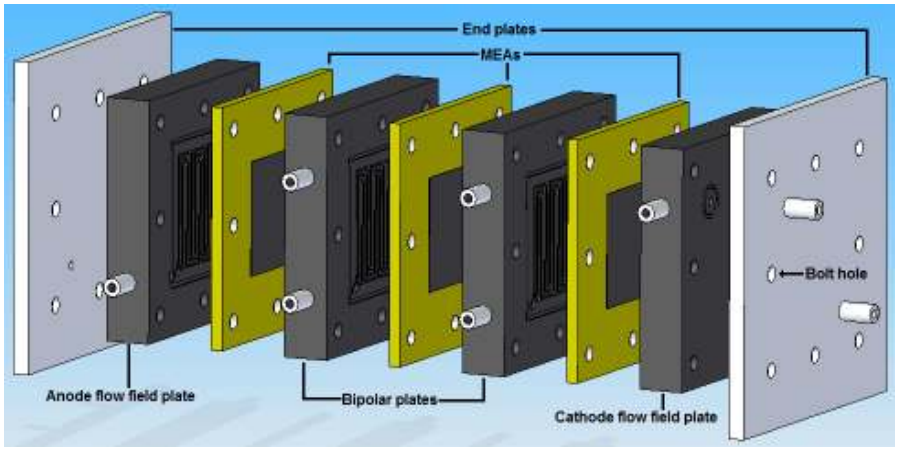

Figure 22 Exploded view of the RFC

Figure 23 Complete three cell RFC stack

3.5 Water crossover

The water management in the RFC is however mainly concerned with the FC mode. In the RFC mode the diffusion of water molecules results in a significant transfer of water molecules from the anode chamber to the cathode chamber. This water crossover results in an H_2 and H_2O mixture (Larminie & Dicks, 2003:53).

The transport within the perfluorinated membrane is complex; the migration of each proton in the membrane is linked to the transport of at least one water molecule. The water molecule moving from the anode to the cathode transports the proton as a hydronium molecule. The transportation of the H_2 by the water molecule is known as electro-osmotic drag (Hoogers, 2003:4-13). According to Hoogers (2003) the number of water molecules used to perform this action varies between 0.6 and 2.0.

In the FC mode the electro-osmotic drag, the production of water at the O_2 electrode and the uptake and evaporation of water molecules give rise to what is known as water back diffusion. Back diffusion acts in the opposite direction to the electro-osmotic drag and results in a water balance at the equilibrium conditions within the FC mode. When the load is increased the equilibrium is shifted and can result in two major phenomena namely drying out and flooding of the MEA. Thus the management of hydration levels within the RFC in FC mode is critical (Larminie & Dicks, 2003:53).

If flooding or drying out of the MEA in the FC mode occurs it will cause a decrease in performance or can even cause the destruction of the MEA. Flooding occurs when the pores

of the catalyst layer are flooded and causes a higher mass transport resistance. Drying out occurs when there is insufficient water inside the MEA; this causes a higher ionic resistance and larger ohmic losses which causes a substantial drop in cell potential (Mengbo & Zidong 2009). Buchi and Srinivasan (1997) confirmed a long-term MEA performance degradation under operation conditions of zero external humidification: after 1200 hours life tests the current density dropped from 1.7 to 1.3 $mA.mm^{-2}$ at constant potential of 0.61 V.

3.6 Water trap

In order to ensure the H_2 produced by the RFC contains no water owing to the water crossover a water trap was designed. The key requirements of the water trap are:

- Trap the water formed at the cathode chamber;
- Automatically drain the water in the water trap;
- Water trap must have no leaks;
- Must be able to withstand pressures of up to 1000 kpa.

The HOGEN GC hydrogen generator's water trap is constructed out of steel, which makes it costly and time-consuming to construct. In order to make the water trap cheaper and faster to construct, perspex was used in the design of the water trap for the RFC. The perspex tube had an outer diameter of 50 mm and an inner diameter of 46 mm. The caps on each side of the tube were 6 mm perspex milled with a Roland CNC machine to fit onto the tube. On the top cap two holes were made for an input and output pipe. On the bottom cap one hole was made for the water drain pipe. The water trap design is seen in Figure 24 and was tested to a pressure of 1000 kpa.

The constructed water trap for the RFC and the water trap used in the HOGEN hydrogen generator work in the same manner. The water trap's input pipe is the H_2 and H_2O mixture input. When the H_2 fills the chamber the water will be in the bottom of the water trap. The output pipe of the water trap will enable the H_2 to exit the chamber. The H_2 will contain no water because the water will remain in the bottom of the water trap. The water drain output can be connected to a valve which will remain closed. During the operation of the RFC the amount of water inside the water trap will increase. When the water inside the water trap must be drained the valve is opened and the pressure inside the chamber is used to force the water out through the water drain pipe. When the valve is closed the H_2 will not be able to exit through the water drain pipe. Figure 25 shows the block diagram of the water trap connected to a valve. This will enable the system to automatically drain the water inside the

water trap controlled by the PLC. The valve will open automatically every 10 min in order to drain the water.

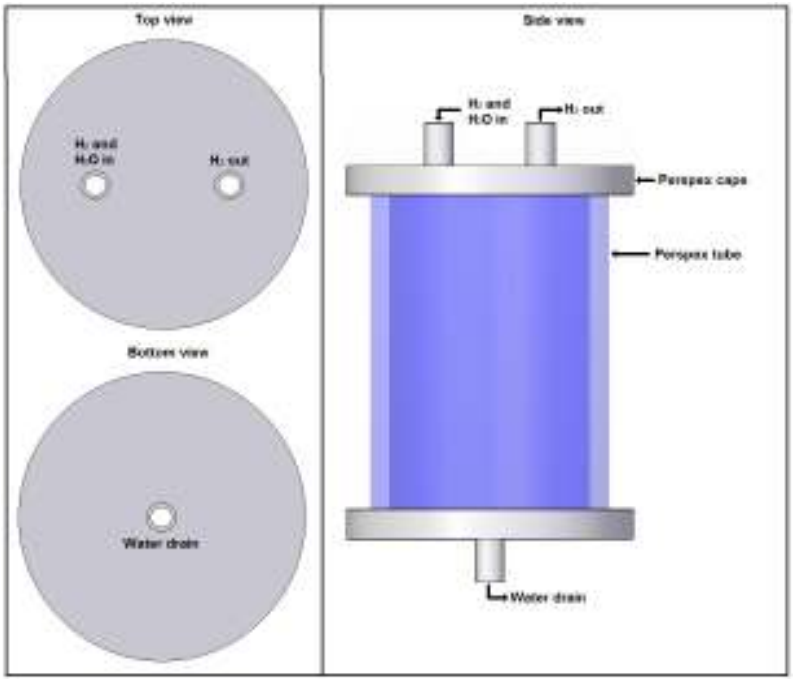

Figure 24 Water trap design

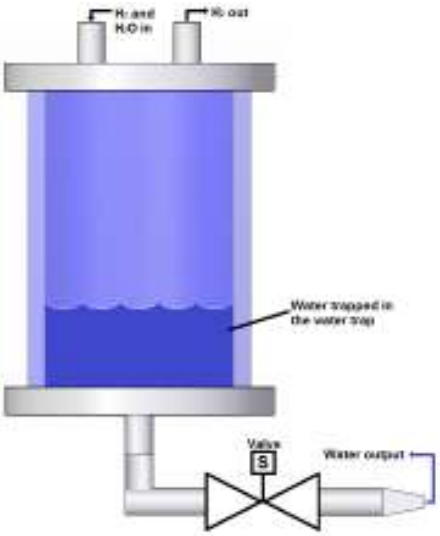

Figure 25 Water trap with valve

The water trap was implemented with the RFC and worked well. Figure 26 shows the water trap built into the RFC test rig.

Figure 26 Water trap built into the RFC test rig

3.7 PLC

ABB's programmable logic controller (PLC) is going to be used to control the optimal operation of the RFC system. It was decided to use the PLC because of two reasons namely firstly the programing of the module is much faster than with other controllers (e.g. PIC microcontroller). The other reason is the PLC has a function that data inside the PLC can be displayed visually (e.g. graphs, charts, etc.) on the PC. The Continuous Function Chart (CFC) programing language is going to be used to programme the PLC in order to control the optimised aspects of the RFC system. These aspects include:

- Control of the supply voltage to the RFC ;
- Automatically drain the water inside the water trap ;
- Control the water flow ;
- Control the temperature of the RFC.

The PLC that is used is a midrange controller (PM554). The controller has seven digital inputs and five digital outputs; an expansion module (AX521) is connected to the controller to add four analog inputs and outputs.

3.8 Summary

In this chapter the various design parameters were given, this included the different dissections of the components of the RFC. The different components required to build the

three cell RFC were designed and manufactured. When all the components were complete the three cell RFC was constructed. The water hydrogen phenomena were investigated and owing to this a water trap was designed and constructed to eliminate the water in the hydrogen owing to the water crossover. The control method that will be used for optimising the RFC operating process was also given

In Chapter 4, the experimental setup to optimise the operation of the RFC will be given. The parameters to optimise are the stack voltage, water supply and the temperature of the RFC.

Chapter 4 Measurements and results

4.1 Introduction

This chapter gives an overview of all of the experiments performed on the designed RFC. The methods followed and results obtained for each experiment are also given. The experiments chosen to be performed on the RFC helped to optimise the operation of the RFC. The optimised RFC can be used in an SHS as explained in Chapter 1. All the experiments were performed on a three cell RFC stack.

4.2 Experimental setup

A RFC test rig was constructed in order to conduct a number of experiments. The block diagram of the experimental setup can be seen in Figure 27. The water trap and the RFC is shown in Figure 28. The stack voltage of the RFC was supplied by a 15 V 10 A bench power supply. One of the hydrogen outlets was blocked off because both hydrogen outlets are linked together.

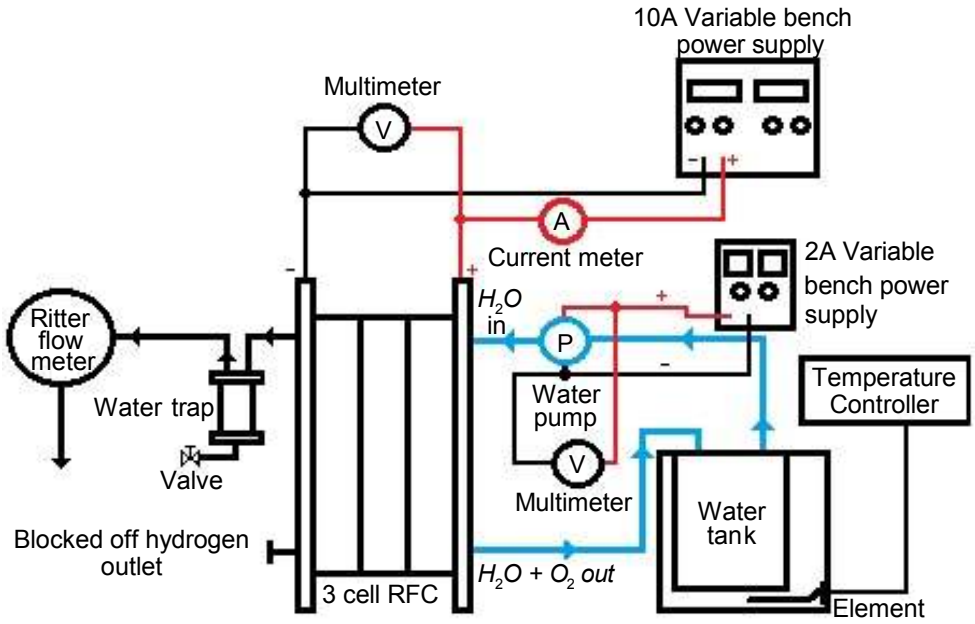

Figure 27 Block diagram of the experimental setup

There are mainly four types of water-heating methods namely:

- Internal electrical coiled type - It has an electrical coil placed inside the storage tank that allows for heating of a large quantity of water with amazing recovery rates.

- External submerged type - Consists of copper tubes that are protected by a stainless steel or cast iron shell. There is a need for an external heat exchanger that uses one pump each for water and for heat transfer.
- Furnace-based type - In this system the heat exchanger coil circulated water through the boiler/furnace so that it could be heated and then sent to a storage tank for use.
- Tank-in-tank type - This type of an indirect-fired water heater is made of two tanks; the inside and the outer tank. The liquid in the outer tank is used to warm the liquid in the inner tank. The Weil McClain indirect water heaters are good examples of tank-in-tank heaters. This is a highly effective water heating system as this design is three times more capable than an electric water heater, and two times more capable than a tank less coil water heater.

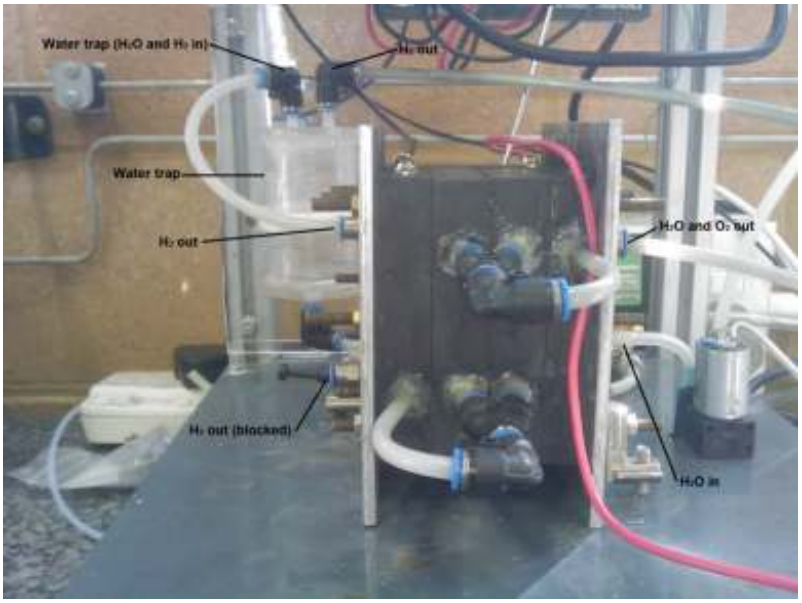

Figure 28 RFC and the water trap

The indirect tank-in-tank water heating method was used to heat the distilled water for the RFC. The reason for this is if an element or metal pipes are used to warm the distilled water directly as the water could become contaminated it and the tank-in-tank method is highly effective. If the distilled water is contaminated the MEA of the RFC will be damaged and its lifetime will shorten dramatically. The water inside the big water container is warmed to the desired temperature; this will increase the temperature of the distilled water inside the smaller container. This method of warming the distilled water for the RFC will ensure that the water does not become contaminated and harm the MEA of the RFC. Figure 29 shows the indirect tank-in-tank water heating configuration.

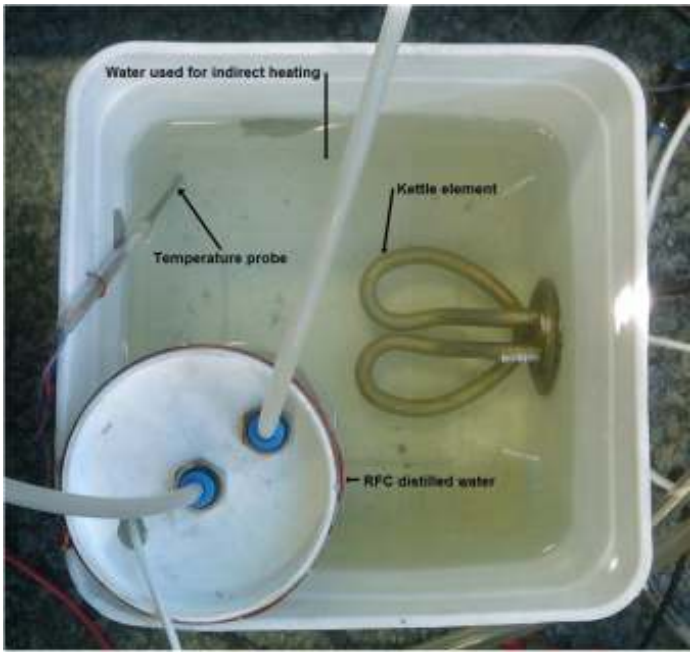

Figure 29 Indirect tank-in-tank water heating

The temperature of the water used to heat the distilled water was controlled by a Carel temperature controller. The desired temperature was set on the controller and the temperature of the water was measured by means of a temperature probe connected to the Carel temperature controller seen in Figure 30.

Figure 30 Temperature controller

If the temperature of the water is less than the temperature set on the controller it will switch a relay to its on state; however if the temperature of the water goes below the desired temperature the relay will be switched to its off state. If the relay is in its on state the element circuit will be complete, this will ensure current flow through the element and will warm the water. If the relay is in its off state the element circuit will not be complete and there would be no current flow. The circuit for the controller is shown in Figure 31.

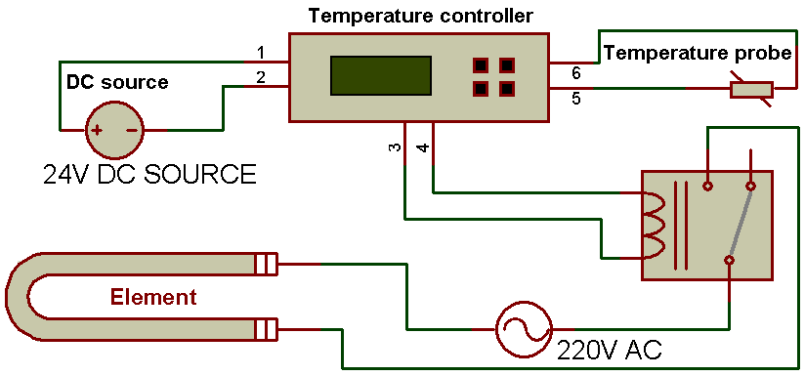

Figure 31 Element circuit

The distilled water is pumped through the RFC with the help of a small water pump (by Flodos) seen in Figure 32.

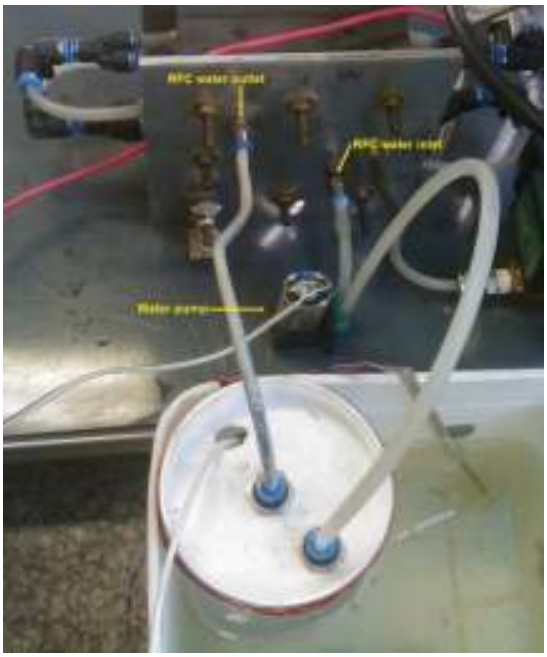

Figure 32 Water supply to the RFC

The water pump is a 12 V pump and is able to supply a maximum flow rate of 0.1 l/min. The pump also has an excellent chemical resistance (Annexure B). The flow rate of the pump can be controlled by adjusting the supply voltage to it. The pump's inlet is connected directly to the distilled water container. The outlet of the pump is fed into the RFC water inlet, the water oxygen mixture exits at the RFC water outlet and returns to the distilled water container. The flow rate of the hydrogen produced by the RFC was measured by using a gas Ritter drum type flow meter shown in Figure 33.

Figure 33 Ritter flow meter

"Ritter drum-type gas flow meters are universally applicable for measuring the volume of flowing gases and are particularly effective when measurements demand the highest precision. The measurement of Ritter drum-type gas meters works on the principle of displacement. The gas meters contain a revolving measuring mechanism (measuring drum) within a packing liquid (usually: water or thin-bodied oil). The measuring drum compulsorily measures volume by periodically filling and emptying four rigid measuring chambers. Fastidious production methods and calibration enable a measuring accuracy of ± 0.2 % at standard flow rate and approx. ± 0.5 % over the whole measuring range. The major advantage and the superiority of volumetric gas meters (like drum-type gas meters) over other measurement principles, which determine gas volume by using secondary measurable variables such as speed, heat capacity, hot-wire resistance or similar, is that the volume of the gas is directly measured. That means that the condition and the composition of the gas have no influence on the measurement accuracy. Correcting factors which take into account gas type, temperature, humidity etc. are therefore not necessary. It should be noted that with

other non-volumetric measurement processes, the measurement accuracy given for that process can only be achieved if the correcting factors for the immediate condition of the gas are exactly known" (Annexure C).

The specifications for the Ritter flow meter used for these experiments are as follow:

Table 5. Ritter specifications

Ritter	
Type	TG 1/5
Min flow rate	2 l/h
Max flow rate	120 l/h
Max pressure	50mbar

The hydrogen output of the RFC was connected to the Ritter flow meter to determine the flow of hydrogen produced. A stop watch was used to time how long it takes for 0.3 liter (l) of hydrogen gas to pass through the meter. The following formula was used to determine the flow of hydrogen produced:

$$l/h = \left(\frac{60}{\frac{t}{3}} \times 0.1 \right) \times 60 \qquad (10)$$

Where:

l/h ≡ liter per hour hydrogen

t ≡ time it takes for 0.3 l of hydrogen to pass through the flow meter

4.3 Stack voltage

The aim of this experiment is to determine the optimised stack voltage of the RFC. The setup for this experiment was done with the following equipment and is shown in Figure 34:

- Water pump
- 2 A Variable bench power supply
- 10 A Variable bench power supply
- Digital multimeter
- Current meter

- Ritter flow meter
- Stop watch
- Distilled water
- Water trap

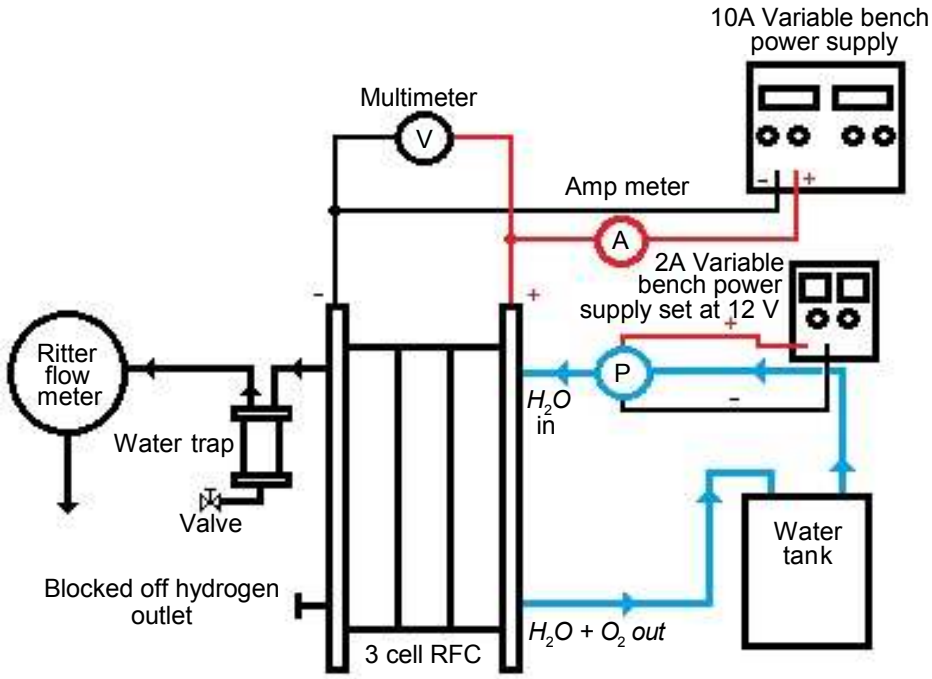

Figure 34 Stack voltage experimental setup

The water pump supplied the RFC with distilled water. The temperature of the water passing through the RFC was kept constant at 34ºC. The temperature of the RFC used in this experiment can be any temperature (in its operating range) but it must be kept constant, because the temperature has an effect on the current and flow of H_2 produced. A constant voltage of 5.1 V was supplied to the RFC for a time period of 5 min in order for the stack current to stabilize. A voltage of 5.1 V was chosen because if the minimum voltage were applied the current would not stabilise because the voltage is less than the required RFC decomposing voltage. The voltage of each cell is measured between two adjacent bipolar plates. The stack voltage is measured between the anode and cathode supply connection to the bipolar plate. A current meter is connected in series to confirm that the reading on the power supply is correct. Then the voltage after 5 min is decreased to the minimum voltage used for this test that is 3.94 V. The stack voltage is increased by 0.15 V increments that result in the increase of a cell voltage of 0.05 V. After each time the voltage is increased it is left for 5 min before the measurements are taken; this is done in order for the current to

stabilise. Table 6 shows the results obtained from the experiment. Figure 35 shows the graphical representation of the flow of H_2 produced vs. voltage and current vs. the voltage. All the values for the graphs were obtained from Table 6.

Table 6. Stack voltages

Stack Voltage (V)	Voltage per Cell (V)	Stack Current (A)	Temperature (ºC)	Flow (l/h)
3.94	1.3	0.0	34	0.0
4.07	1.35	0.0	34	0.0
4.21	1.4	0.2	34	0.0
4.34	1.45	0.6	34	0.0
4.5	1.5	1.5	34	1.9
4.65	1.55	2.8	34	4.2
4.83	1.6	4.5	34	7.1
5.05	1.65	5.7	34	9.5
5.25	1.7	6.9	34	11.4
5.38	1.75	7.5	34	12.4
5.5	1.8	8.2	34	13.5
5.65	1.85	9.0	34	14.8
6	1.9	10.2	34	15.7
6.06	1.93	11.0	34	17.2

The efficiency of the RFC at STP can be calculated using the following equation (Doddathimmaiah, 2006:52-55):

$$\eta^E = \frac{E_{hydrogen}}{E_{electric}} \times 100\ \%$$

$$\eta^E = \frac{V_{H2}.HVV}{V.I.t} \times 100\ \% \qquad (11)$$

Where:

η^E ≡ Efficiency of RFC (%)

V_{H2} ≡ The flow rate of H_2 produced in mole

HVV ≡ Higher heating value of hydrogen (142 MJ/kg at 25°C)

V ≡ RFC supply voltage (V)

I ≡ Current drawn by the RFC (A)

t ≡ Time in seconds (s)

To do the calculations for efficiency the flow rate must be converted from l/h to mole/h. At STP 1 mole of gas is equal to 22.4 l. The time must also be converted into seconds, 1 hour equals 3600 seconds. The RFC efficiencies of the different stack voltages were calculated using the data in Table 6. Shown below is an example of the calculation done for the stack voltage of 5.05 V :

$$\eta^E = \frac{V_{H2}.HVV}{V.I.t} \times 100\ \% \tag{12}$$

$$\eta^E = \frac{(0.42)(1.42 \times 10^3)}{(5.05)(5.7)(3600)} \times 100\ \%$$

$$\eta^E = 56.85\ \%$$

The efficiency of the different stack voltages is shown in Table 7. The graph of the efficiency vs. voltage and current vs. voltage is shown in Figure 36. As seen in Figure 36 the efficiency peaked at a stack voltage of 5.05 V. If a stack voltage is greater or less than 5.05 V the efficiency of the RFC will decrease.

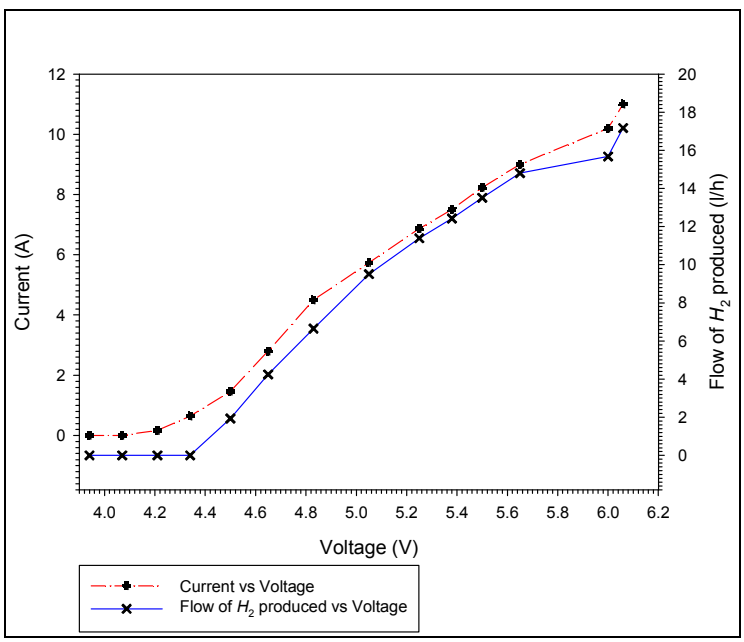

Figure 35 Flow of H_2 and current vs. stack voltage

Table 7. RFC efficiency data

Stack voltage (V)	Stack current (A)	Flow (mol/h)	Efficiency (%)
3.94	0	0	0
4.07	0	0	0
4.21	0.2	0	0
4.34	0.6	0	0
4.5	1.5	0.08	46.75
4.65	2.8	0.18	54.56
4.83	4.5	0.31	56.26
5.05	5.7	0.42	56.85
5.25	6.9	0.51	55.53
5.38	7.5	0.55	53.77
5.5	8.2	0.60	52.48
5.65	9.0	0.66	51.2
6	10.2	0.70	45.12
6.06	11.0	0.77	45

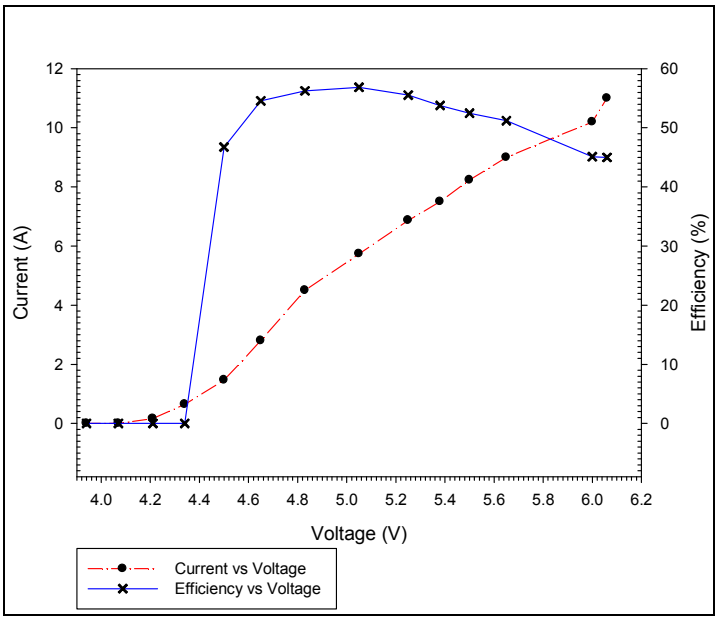

Figure 36 Efficiency and current vs. voltage of the RFC

4.4 Water supply

The aim of this experiment is to determine what effect the water flow rate through the RFC has on the flow of H_2 produced by the RFC. The setup for this experiment was done with the following equipment and is shown in Figure 37:

- Water pump
- Distilled water
- Multimeter
- Current meter
- 2 A Variable bench power supply
- 10 A Variable bench power supply
- Ritter flow meter
- Stop watch
- Water trap

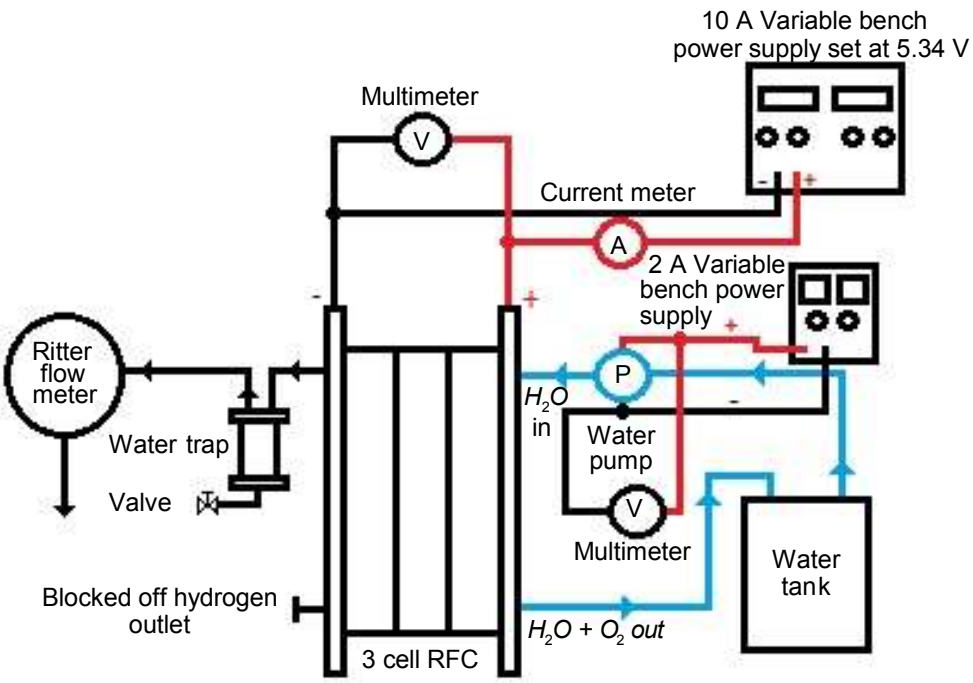

Figure 37 Water supply experimental setup

The flow rate of the water pump can be changed by changing the supply voltage to the pump. The minimum supply voltage was 5 V and was increased in 1 V increments to a maximum voltage of 12 V. The supply voltage could only be varied between 5 V and 12 V as

this was the operating voltage limitations to the pump used. Table 8 and Figure 38 show the relationship between the supply voltage to the pump and the flow rate of H_2O.

Table 8. Relationship between pump supply voltage and H_2O flow rate

Pump supply voltage (V)	H_2O flow rate (ml / min)
5	26.5
6	36.58
7	46.15
8	53.57
9	50
10	36.83
11	73.17
12	76.92

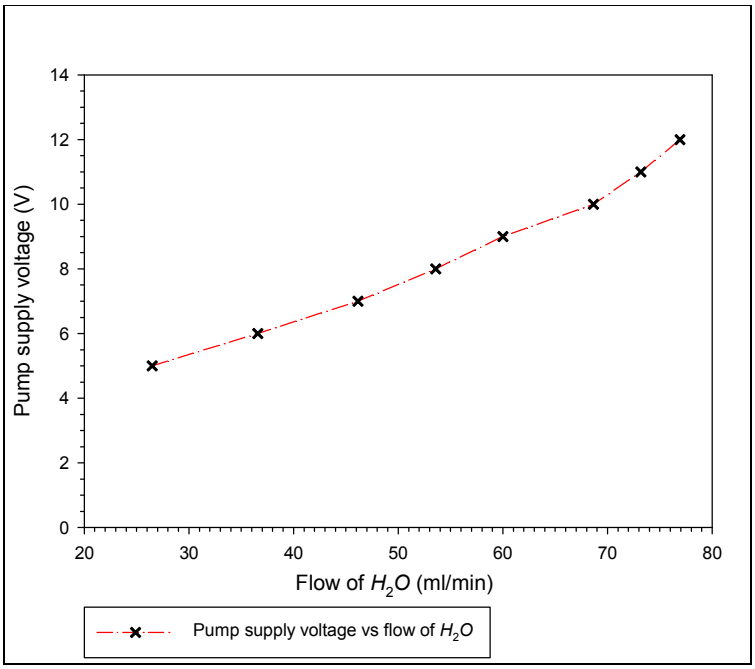

Figure 38 Pump supply voltage vs. flow rate of H_2O

It can be seen that the minimum and maximum flow rate was 26.5 ml/min and 76.92 ml/min respectively. The voltage of the pump was set to 5 V in order to pump water through the RFC at a rate of 26.5 ml/min thus a constant voltage of 5.05 V was supplied to the RFC. A

voltage of 5.05 V was chosen because it is the optimal operating voltage for this RFC. After each time the flow rate of the water pump was adjusted a waiting period of 5 min was allowed to determine if there is a change in current drawn by the RFC or flow of H_2 produced.

The temperature was also kept constant at 34°C. The temperature of the RFC used in this experiment can be any temperature (in its operating range) but it must be kept constant, because the temperature has an effect on the current and flow of H_2 produced. At each different flow rate of H_2O, measurements were taken over a time period of 30 min in order to obtain the average flow of H_2 produced. Table 9 shows the results for this experiment and Figure 39 shows the graphical representation of the flow rate of H_2O and pump voltage vs. flow rate of H_2 produced.

The results showed that the flow of H_2 produced was constant throughout the experiment. Thus the conclusion can be made that the flow rate of H_2O did not have an effect on flow of H_2 produced. Thus it is not necessary to control or optimise the water flow on this RFC, because it has no effect on the flow of H_2 produced.

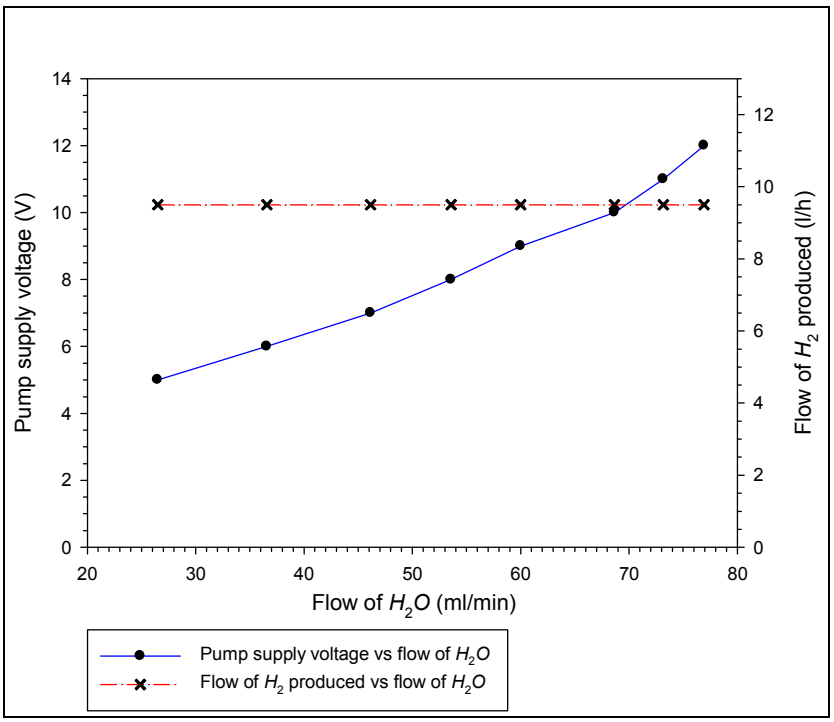

Figure 39 Flow rate of H_2 and pump voltage vs. Flow rate of H_2O produced

Table 9. Flow rate of H_2O vs. flow rate of H_2 produced

Flow rate of H_2O (ml / min)	Voltage of RFC (V)	Current of RFC (A)	Average Flow of H2 produced (l / h)
26.5	5.05	5.7	9.5
36.58	5.05	5.7	9.5
46.15	5.05	5.7	9.5
53.57	5.05	5.7	9.5
50	5.05	5.7	9.5
36.83	5.05	5.7	9.5
73.17	5.05	5.7	9.5
76.92	5.05	5.7	9.5

4.5 The effect of temperature on the RFC

The aim of this experiment is to determine the effect that the temperature has on the production of H_2 by the RFC. The setup for this experiment was done with the following equipment and is shown in Figure 40:

- Water pump
- Distilled water
- 2 A Variable bench power supply
- 10 A Variable bench power supply
- Digital multimeter
- Current meter
- Ritter flow meter
- Stop watch
- Indirect tank-in-tank water heating method
- Carel temperature controller
- Water trap

The Carel temperature controller was set to the desired temperature in order to switch the element in such a way so as to increase the temperature of the water used for the indirect water heating to the desired temperature. The distilled water temperature will also then increase to the same temperature of the water used for the indirect water heating. The temperature of the distilled water at the beginning of the experiment was close to room

temperature that was 20ºC. The distilled water was pumped through the RFC at a constant rate and a constant stack voltage of 5.34 V was applied on the RFC. The supply voltage of this experiment can be any voltage within the RFC operating voltage limits (4.5 V to 6.06 V) but must be kept constant because the voltage has an effect on the current and the flow of H_2 produced.

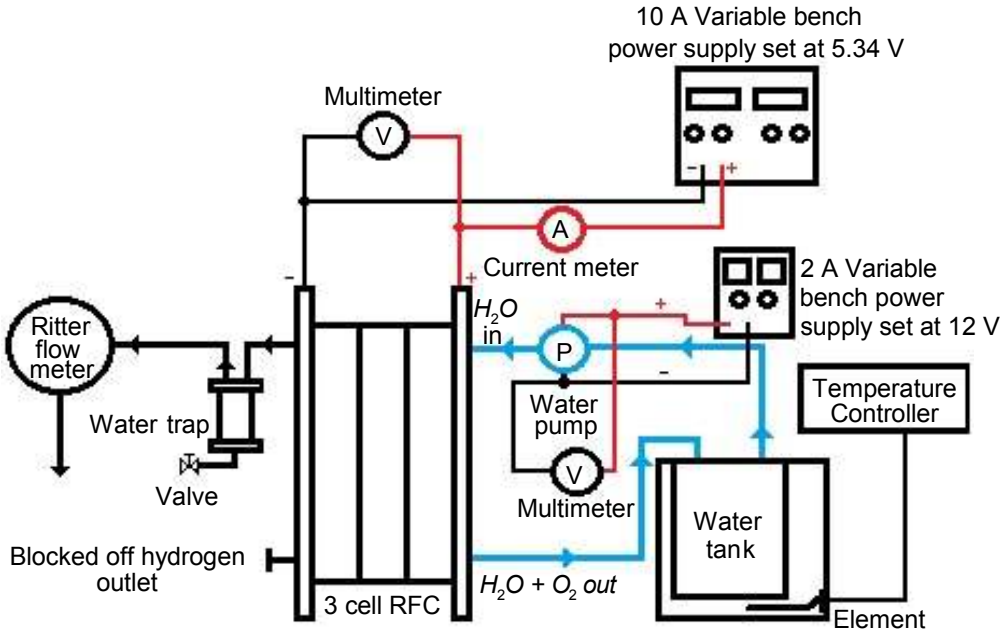

Figure 40 Temperature experimental setup

After the voltage was applied to the RFC it was left for 5 min in order for the current to stabilise. After 5 min the first measurements were taken for 20ºC then the Carel temperature controller was set to 30ºC. The warming of the distilled water was a time-consuming process. When the distilled water reached 30ºC the second measurements were taken. The temperature was increased by increments of 10ºC each time until it reached 70ºC. A temperature of 70ºC was the maximum temperature that could be tested because the plastic containers used were close to melting point. The measurements recorded included the current drawn by the RFC at 5.34 V and the flow of H_2 produced. The results of the experiments are given in Table 10; from the data in the table two graphs were plotted which includes current vs. temperature seen in Figure 40 and flow of H_2 produced vs. temperature seen in Figure 42.

It is clearly noted that an increase of temperature will increase the current drawn by the RFC (shown in Figure 41). When the current drawn by the RFC increases the flow of H_2

produced also increases. Thus the conclusion can be made that if the operating temperature of the RFC is increased the flow of H_2 produced will also increase although the stack voltage remained constant.

Table 10. Effect of temperature

Temperature (ºC)	Voltage of stack (V)	Current of stack (A)	Flow of H_2 produced (l/h)
20	5.34	6.5	11.02
30	5.34	8	14.02
40	5.34	9.7	16.36
50	5.34	11.3	20
60	5.34	12.3	21.6
70	5.34	13.3	22.98

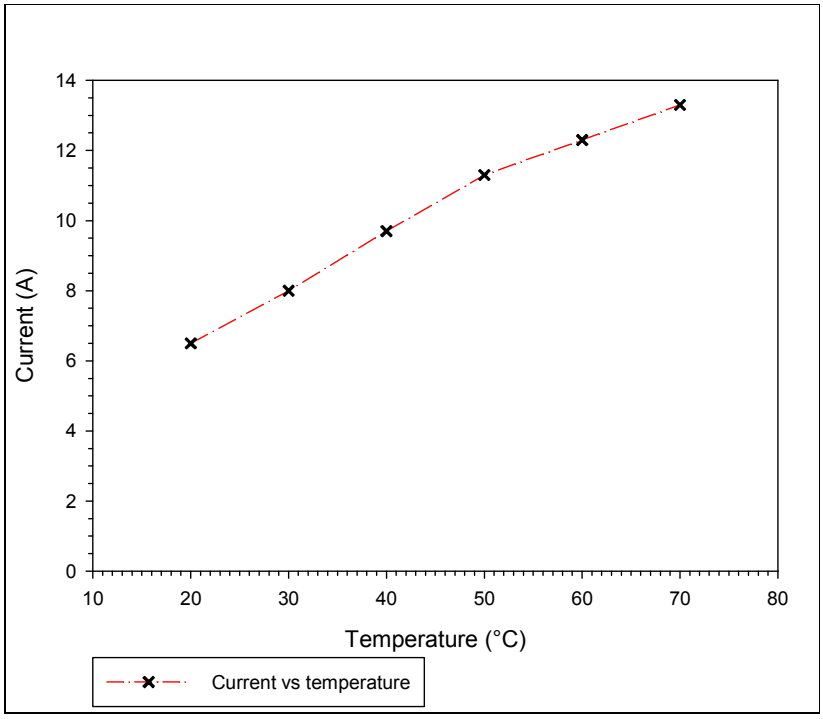

Figure 41 Current vs. temperature

If the operating temperature of the RFC is increased it must be kept in mind that the amount of energy it takes for the RFC to reach its desired temperature can decrease the overall RFC

system's efficiency. If the RFC is used for a SHS (as discussed in Chapter 1) the amount of power used on the warming of the RFC must not be greater than the amount of power one gets from the extra hydrogen produced. In order to calculate the amount of power it takes to warm 1 l of water to a certain temperature the following equation is used (Joel, 1996:20-23)

$$Q = c_p m dT \tag{13}$$

Where:

Q ≡ amount of power (kJ)

c_p ≡ specific heat constant of water 4.19 $kJ / kg^{o}C$ ($kJ / kg^{o}C$)

m ≡ mass of liquid (kg)

dT ≡ temperature difference between start and end temperature (ºC)

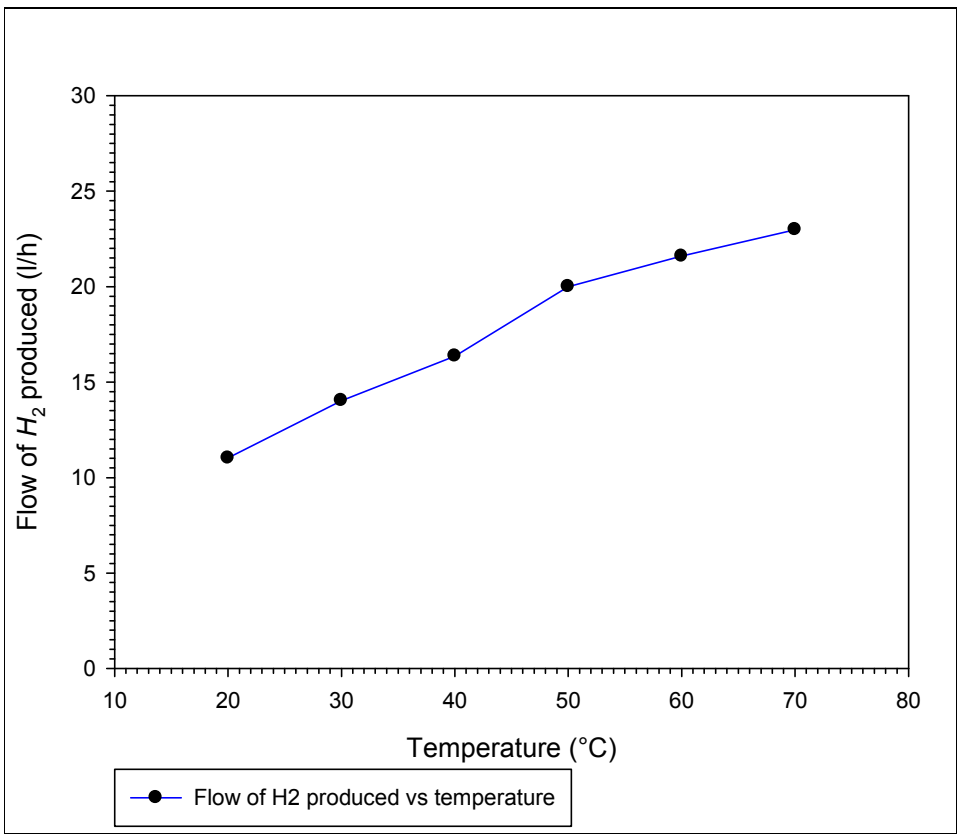

Figure 42 Flow of H_2 produced vs. temperature

The starting temperature for the following equations will be lab temperature which in this case is 20ºC. Three calculations were done raising the temperature from 20ºC to 30ºC, 50ºC

and 70ºC. In these calculations 1 l of water was warmed (**note:**1 l water has a mass of 1 kg).

$$Q_{30} = c_p mdT \tag{14}$$
$$Q_{30} = (4.19)(1)(30-20)$$
$$Q_{30} = 41.9 \text{ kJ}$$

$$Q_{50} = c_p mdT \tag{15}$$
$$Q_{50} = (4.19)(1)(50-20)$$
$$Q_{50} = 125.7 \text{ kJ}$$

$$Q_{70} = c_p mdT \tag{16}$$
$$Q_{70} = (4.19)(1)(70-20)$$
$$Q_{70} = 209.5 \text{ kJ}$$

The amount of power in kJ can be converted into W.h with the following equation:

$$J = W \times 3600 \tag{17}$$

Where :

J ≡ Amount of power in Joule

W ≡ Amount of power in Watt

Therefore:

$$J_{30} = W \times 3600 \tag{18}$$
$$W = \frac{41900}{3600}$$
$$W = 11.64 \text{ W.h}$$

∴ For each hour 11.64 W is consumed

$$J_{50} = W \times 3600 \tag{19}$$
$$W = \frac{125700}{3600}$$
$$W = 34.92 \text{ W.h}$$

∴ For each hour 34.92 W is consumed

$$J_{70} = W \times 3600 \tag{20}$$

$$W = \frac{209500}{3600}$$

$$W = 58.19 \text{ W.h}$$

$\therefore$ For each hour 58.19 W is consumed

4.5.1 NEXA® Power Module

The next experiment is done to determine the amount of power that can be generated by using hydrogen with a flow rate of 1 l/h by the Nexa® Power Module. "The Nexa® Power Module comprises of an air-cooled fuel cell stack using Billard's approved PEM technology. Using hydrogen and oxygen (from ambient air) as fuel it can generate up to 1200 W of unregulated DC power". The design of the Nexa® Power Module (specifications in Annexure D) is well suited for a variety of applications such as:

- Stationary power supply systems,
- Backup power generators,
- Recreational and portable products.

The Nexamon® OEM control software (specifications in Annexure D) can be seen in Figure 43.

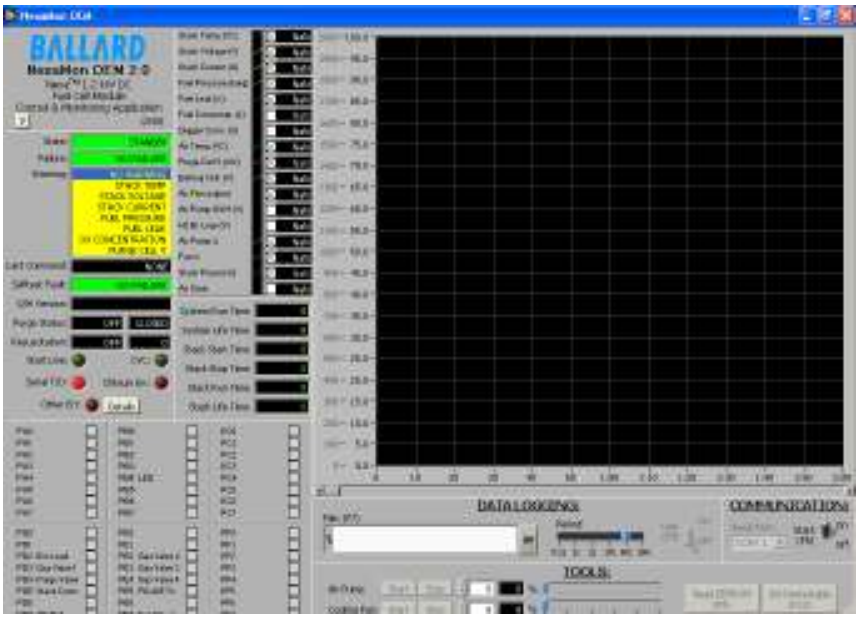

Figure 43 Nexamon® OEM control software

The Nexamon® OEM control software allows the user to set parameters and monitor operational data such as:

- Stack voltage, current and temperature,
- Hydrogen pressure and consumption,
- Ambient temperature,
- Air mass flow rate,
- System operating time.

The Nexa® Power Module was connected to a DC load in order to determine the hydrogen usage. The Nexamon® OEM control software was used to monitor the hydrogen consumption of a 100 W load. Figure 44 shows the block diagram of the Nexa experiment setup.

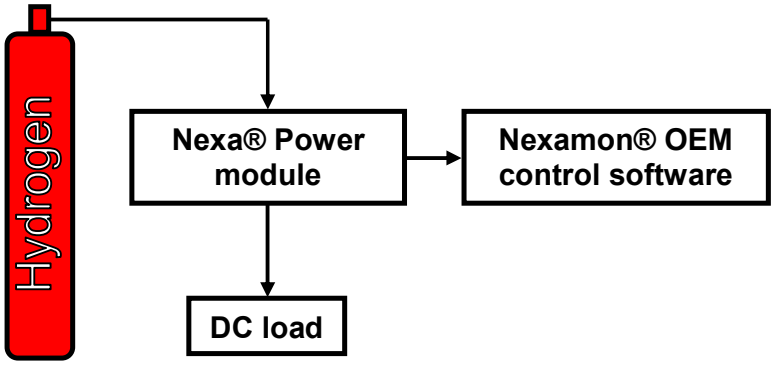

Figure 44 Experiment setup with Nexa® Power Module

The result obtained in this experiment is given in Table 11. The Nexa® Power Module supplied power to the 100 W load for one hour.

Table 11. Hydrogen consumption

Load (W)	Fuel consumption (l/h)
100	72

From the data obtained in Table 11 the following calculation is done to determine the maximum load that can be connected to the FC if there is a hydrogen flow rate of 1 l/h (As shown in Table 11: For a 100 W load the Nexa® Power Module consumed 72 l/h).

$$\frac{\text{Load}}{72} = \frac{\text{Fuel consumption}}{72} \tag{21}$$

$$\frac{100}{72} = \frac{72}{72}$$

$$1.38\ \text{W} = 1\ \text{l/h}$$

As seen in the calculations a hydrogen flow rate of 1 l/h can supply a maximum load of 1.38 W with power. The comparison between the amount of extra power that can be produced when the RFC's temperature is increased and the amount of power to warm the RFC is given in Table 12.

Table 12. Energy that is generated by the extra hydrogen

30ºC	**50ºC**	**70ºC**
It takes **11.64** W (for one hour) to warm the water from 20ºC to 30 ºC	It takes **34.92** W (for one hour) to warm the water from 20ºC to 50ºC	It takes **58.19** W (for one hour) to warm the water from 20ºC to 70ºC
Seen in the data in Table 10 there was a **3** l/h improvement in hydrogen production	Seen in the data in Table 10 there was a **9** l/h improvement in hydrogen production	Seen in the data in Table 10 there was an **11** l/h improvement in hydrogen production
The extra power that can be produced with the extra hydrogen is **4.14** W	The extra power that can be produced with the extra hydrogen is **12.42** W	The extra power that can be produced with the extra hydrogen is **15.18** W

As seen in Table 12 the power that is consumed by the warming process for the RFC is more than the amount of power that the extra hydrogen can produce. Thus if the RFC's temperature is increased in order to produce more hydrogen the input power (warming the RFC) will be more than the output power of the extra hydrogen. This will decrease the efficiency of the SHS dramatically. Thus it was decided not to warm the RFC because it would decrease the overall RFC efficiency.

4.6 The optimised RFC system

As mentioned in Chapter 3 the aspects that need to be controlled are the water flow, temperature, supply voltage to the RFC and draining of the water inside the water trap, but as seen in the experiments addressed in this chapter there is no need to control the water

flow as it has no effect on the hydrogen produced. The operating temperature of the RFC has an effect on the hydrogen produced but the RFC must not be warmed as it consumes more energy to warm the RFC than one gets from the extra hydrogen produced. The RFC stack voltage is optimised at 5.05 V; if a greater or lesser stack voltage is applied the efficiency of the RFC decreases.

Thus two aspects of the RFC system that is controlled by the PLC to optimise the operation, is the switching of the RFC stack voltage and the control of the water release valve for the water trap. The switching of RFC supply voltage was done by connecting a relay to the PLC. The control water release valve for the water trap was done by connecting the valve to the PLC's digital output. If there is an error in the system or the hydrogen pressure has reached the desired output of hydrogen the relay will then switch which will break the RFC supply circuit. If the relay switched there will not be a supply voltage to the RFC and it will therefore not produce any more hydrogen. The block diagram of the PLC control system used to optimise the RFC system is shown in Figure 45.

The programing in Codesys of the RFC stack voltage relay circuit is shown in Figure 46. The variables must have the following values otherwise the relay will switch: System_stop must be a logic 0, On_button must be a logic 1 and the over_pressure must be a logic 1. The System_stop will have a logic 1 if there is a system error. If the On button is pressed in the visual form On-button will be a logic 1 but if the Off button is pressed On_button will have a logic 0, and over_pressure will be a logic 1 if the hydrogen pressure has not reached the desired output pressure but will be a logic 0 if the hydrogen pressure reached the desired output hydrogen pressure. The visual form for the PLC can be seen in Figure 47.

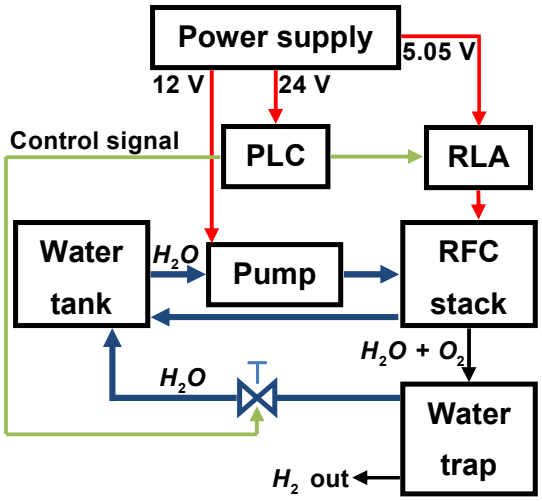

Figure 45 PLC control block diagram

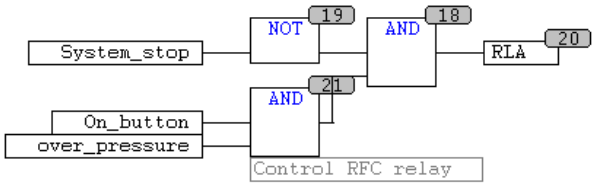

Figure 46 Relay Codesys programming

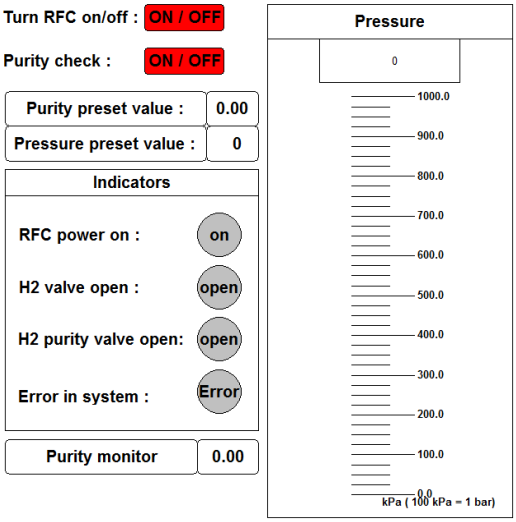

Figure 47 Visual form

Figure 48 shows the programming of the water release valve in Codesys. Before the water release valve program will be enabled the RLA variable (supply voltage to the RFC) must be a logic 1. When the RLA variable is a logic 1 the Water_timer will give a delay of 10 min before switching the water valve output to high and when water output is high water_timer_2 will reset the process in 1ms.The wave form for the water release valve is shown in Figure 49.

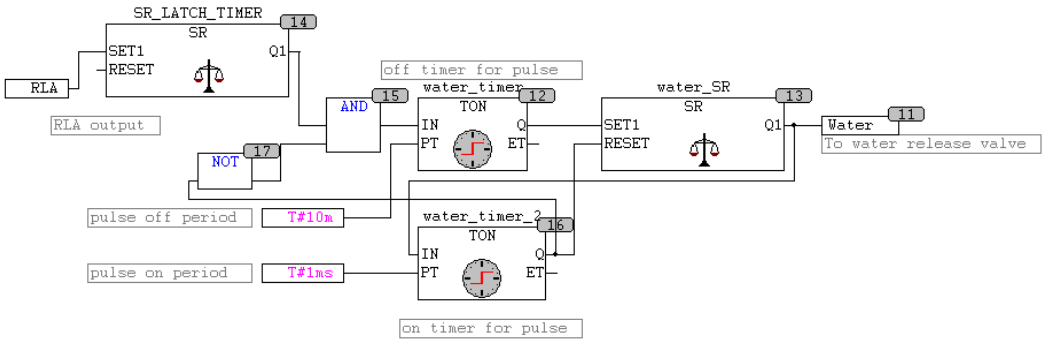

Figure 48 Water release valve Codesys programming

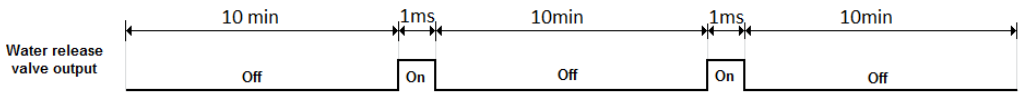

Figure 49 Water release valve output wave form

The entire optimised RFC system which can produce hydrogen at a desired pressure is shown in Figure 50. The building of the RFC system involved the research addressed in this document as well as the research of Ms M Burger a fellow student.

Figure 50 Hydrogen generator

4.7 Summary

In Chapter 4, the experimental setup on which all the necessary experiments were performed to optimise the voltage, temperatures and water management of the RFC was given. It was found that if the stack voltage were at 5.05 V the efficiency of the RFC was the highest at 56.85 %. The water flow rate through the RFC had no effect on the flow of

hydrogen produced thus there is no need to control the water flow rate. The temperature of the RFC had an effect on the flow of hydrogen produced, an increase of temperature resulted in a increase of flow of hydrogen produced. However it was found that if the temperature of the RFC were to be increased the efficiency of the system would decrease, thus there is no need to control the temperature of the RFC.

Chapter 5 is the final section in this dissertation. It will deal with the conclusions and recommendations that evolved from the study of the optimisation of water, temperature and voltage management on a RFC.

Chapter 5 Conclusions and recommendations

Introduction

The research to optimise the water, temperature and voltage management of a RFC was carried out and conclusions have been made from the results obtained. The intended objectives were achieved. The recommendations for the future research in the RFC technology will now also be discussed.

5.1 Conclusions

5.1.1 The construction of the RFC

It was found that the design of the RFC centred around the MEA 'the heart' of the RFC. Although the research did not focus on the manufacturing of the MEA, different types of MEAs were considered. A study was made of the type of electrocatalyst that could be used in the MEA for the RFC. The research showed that the *Pt* black cathode electrocatalyst of the Nafion N-115 MEA showed good performance in the FC and RFC modes. However, *Pt* black could not be used for the anode electrocatalyst because it has excellent performance in the FC mode but poor performance in the RFC mode. The literature research also showed that the best electrocatalyst used at the anode is *IrRuOx Pt* black. The *IrPt* black will be the dominant conductor in the RFC mode and will be inactive during the FC when *Pt* black will be active. *RuOx* was used for better conductivity and is also less costly. The research showed that the Nafion N-115 membrane was the best choice to use in a RFC.

Research into the making of bipolar plates used for a RFC showed that the graphite plate was the best material to be used. Different types of flow fields were investigated and it was found that the three continuous serpentine flow field was superior to that of the pin type, straight and parallel type and the single continuous serpentine type flow fields. After the three continuous serpentine flow fields were drawn in the solid edge CAD program, it was milled into the graphite plates by means of a Roland milling machine. The bipolar plates with a three continuous serpentine flow field showed promising results for the RFC. O rings and O ring cord were used as gaskets for the sealing of the RFC stack and showed better results over rubber gaskets. For technical reasons a three cell RFC was constructed and showed promising results. The manufacturing process of the pates was not optimised and was expensive and time consuming but worked well.

5.1.2 Contro l aspects of the RFC

After several experiments were performed on the RFC it was noticed that there was a presence of water in the hydrogen produced. To remove the water from the water hydrogen mixture, a water trap was designed and constructed using a rapid prototyping machine. The water trap was designed in such a way that the water is drained automatically by the control circuit every 10 minutes. The pressure inside the hydrogen system is used to push out the water inside the water trap if the water drain valve opens. The water drain valve for the water trap is controlled by the PLC. The PLC could also be replaced with a microprocessor because the PLC is very expensive.

It was determined that the optimised voltage of a single cell RFC is 1.68 V thus for a three cell RFC the optimised voltage would be 5.05 V. It was noticed that if the current drawn by the RFC increased the hydrogen production also increased. The efficiency of the three cell RFC stack was the highest at 5.05 V. The efficiency was calculated to be 56.85 %. If the voltage were to be increased beyond 5.05 V more hydrogen is produced but the overall efficiency was decreased. Thus the voltage to this three cell RFC must be fixed at 5.05 V for the optimised operating voltage.

It was also found that there was no difference in the RFC performance if the water flow rate were changed. The water flow rate was changed from 26.5 ml/min to 76 ml/min by changing the voltage on the pump. The water flow rate could only be varied between 26.5 ml/min and 76 ml/min as these were the limitations to the pump used. It was proven that there was no difference in the production rate of hydrogen or current drawn by the RFC if the water flow was changed. Thus there is no need to control the water flow in the RFC because it had no effect on the production rate of hydrogen.

The results also showed that the operating temperature of the RFC had an effect on the production of hydrogen or the current drawn by the RFC. It was also found that if the operating temperature of the RFC was increased it improved the flow rate of hydrogen produced and simultaneously an increase current drawn by the RFC. It was proven that if the operating temperature of the RFC was increased, the energy it consumes to warm the RFC it significantly decreases the efficiency of the whole system. Thus the RFC need not be warmed because it consumes significantly more energy to warm the RFC compared to the energy available for later use. There is thus no need to control the temperature for the optimised operation of the RFC. Room temperature of 20°C is adequate. It was also found if the temperature of the RFC is below 0°C it will stop to operate.

5.2 Recommendations

The following recommendations relating to the further development of RFC technology are made.

- Further research could be done on the physical construction of the RFC for example flow fields, bipolar plates, etc. This could increase the efficiency of the RFC and lower the cost.
- All the experiments done on the three cell RFC, for example the optimised supply voltage, water flow and temperature, should be carried out on more cells and cells with a larger MEA area. The results of the bigger RFC stack must then be compared to the results of this document.
- Further research must be done on how to use a RFC in the FC mode. If the RFC can be used in both modes (FC mode and RFC mode) it can be used in the solar hydrogen system explained in Chapter 1.
- An optimised manufacturing process for the bipolar plates could be investigated.
- Further research into the use of an alternative controller, for example, a microprocessor to reduce the cost of the RFC system.

BIBLIOGRAPHY

AKKERMAN, I., JANSSE, N., M., ROCHA, J. & WIJFFELS, R.H. 2002. Photobiological hydrogen production: Photochemical efficiency and bioreactor design. *International Journal of Hydrogen Energy*, 27(11):1195-1208.

AKSAKAL, Z.C. 2007. *Hydrogen production from water using solar cellspowered nafion membrane electrolyzers*. Đzmir Institute of Technology.

BARNES, J.R. & OVERTON, O. 2003. International Power Plugs and Language. [Online]. Available at: <http://www.dbicorporation.com/internat/intpower.htm>. Accessed: 9/04/2010.

BASU, S. 2007. *Recent trends in fuel cell science and technology*. New Delhi; India: Anamaya Publishers.

BUCHI, F.N. & SRINIVASAN, S. 1997. Operating proton exchange membrane fuel cells without external humidification of the reactant gases. *Electrochem, 144(8)*: 2767-2772.

CALLDO, F. 2008. Eskom's power crisis: Reasons, impact & possible solutions. Solidarity.

CHEN, E. 2003. History. *In* HOOGERS, G. ed. *Fuel cell technology handbook.* Florida:CRC press.

DIHRAB, S.S., SOPIAN, K. & ZAHARIM, A. 2008. Membrane and bipolar plates materials for regenerative fuel cells. *World Scientific and Engineering Academy and Society (WSEAS)*, 1:183-188.

DODDATHIMMAIAH, A. K. 2006. *The use of PEM unitised regenerative fuel cells in solar-hydrogen systems for remote area power supply*. School of Aerospace, Mechanical and Manufacturing; RMIT University.

Farmers - Both perpetrators and victims of climate change. [Online]. 2011. October 31. Available at: < http://allafrica.com/stories/201111010326.html>. Accessed: 07/10/2011.

GRIMES, C.A., VARGHESE, O.K. & RANJAN, S. 2008. *Light, water, hydrogen.* New York: Springer Science + Business Media.

GRIGORIEV, S.A., POREMBSKY, V.I. & FATEEV, V.N., 2006. Pure hydrogen production by PEM electrolysis for hydrogen energy. *International Journal of Hydrogen Energy*, 31(2):171-175.

HAUBOLD, H.G., VAD, T.H., JUNGBLUTH, H. & HILLER, P. 2001. Nano structure of NAFION: a SAXS study. *Electrochimica Acta*, 46(10):1559-1563.

HOOGERS, G. 2003. *Fuel cell technology handbook*. 1st ed. Florida: CRC press.

HEINZEL, A., MAHLENDOR, A. & JANSEN, C. 2009. Bipolar plates. *Encyclopedia of Electrochemical Power Sources*, pp 810- 816.

JOEL, R. 1996. *Basic engineering thermodynamics.* 5th ed. England: Pearson Education Limited.

KORDESCH, K. & SIMADER, G. 1996. *Fuel cells and their applications.* Weinham:VCH

LABURN, P. 2010. An ambitious target that needs an action plan: South Africa and climate change. [Online]. Available at: < http://www.petelaburn.com/index.php/multimedia/pdf-articles/south-africa-and-climate-change/>. Accessed : 07/10/2011.

LARMINIE, J. & DICKS, A. 2003. Fuel cell systems explained. Sussex: John Wiley and Sons.

LEDJEFF, K., MAHLENDORF, F., PEINECKE, V. & HEINZEL, A. 1994. Development of electrode/membrane units for the reversible solid polymer fuel Cell (RSPFC). *Electrochimica Acta*, 40(3):315-319.

LEE, C. 2001. Enthalpy of formation and enthalpy of combustion. [Online]. Available at: *<web.me.unr.edu/me372/Spring2001/Enthalpy.pdf>. Accessed:10/06/2010.*

LYNNTECH Inc. 2007. M. Nelson, personal communication. College Station. Texas. USA.

LI, X. & SABIR, I. 2005. Review of bipolar plates in PEM fuel cells: Flow-field designs. *International Journal of Hydrogen Energy*. 30(4):359-371.

MENGBO, J.I. & ZIDONG, W.E.I. 2009. A review of water management in polymer electrolyte membrane fuel cells. *Energies*, 2(4):1057-1106.

MENNOLA, T. 2007. Design and experimental characterization of polymer electrolyte membrane fuel cells. *Power Electronics IEEE*, 22: 670-678.

MOORTHY, VK. 2006. *Reversible hydrogenising the civilization: Fuel cell*. [Online]. Available at: <http://www.vigyanprasar.gov.in/comcom/feature84.htm>. Accessed: 22/03/2010.

MITLISKY, F., WEISBERG, A. H., CARTER, P. H., DITTMAN, M.D., MYERS, B., HUMBLE, R.W. & KARE, J.T. 1999. Water rocket - Electrolysis propulsion and fuel cell power. *In American Institute of Aeronautics and Astronautics Space Technology Conference and Exposition*.

OH, H.H., YOON, Y.S. & PARK, S.G. 2004. The electrical and physical properties of alternative material bipolar plate for PEM fuel cell system. *Electrochimica Acta*, 50(2):777-780.

OLSON, D.W. 2003. *Graphite*. Geological survey minerals yearbook. US government.

RABIH, S., RALLIERES, O., TURPIN, C. & ASTIER, S. Experimental study of a PEM reversible fuel cell. *University of Toulouse – Laboratory LAPLACE*, 1:1-6.

SA, K. 1999. DME set to power-up non-grid image in SA. *Engineering News*. August 6. [Online]. Available at: <http://www.engineeringnews.co.za/topic/nongrid-electricity>. Accessed 12/02/2011.

SWANEPOEL, F.K. 2005. *Design of a unitized regenerative fuel cell system for remote telecommunications applications*. Vanderbijlpark: Vaal University of Technology.

SMITH, W. 2000. The role of fuel cells in energy storage. *Journal of Power Sources*, 86: 74-83.

THOMPSETT, D. 2003. Catalysts for the proton exchange membrane fuel cell. In HOOGERS, G. Fuel cell technology handbook. 7th ed. Florida: CRC Press.

TSUTOMU, O.I. & YOSHINORI, S. 2004. Optimum hydrogen generation and current density of the PEM-type water electrolyser operated only during the off-peak period of electricity demand. *Journal of Power Sources*, 129(2):229-337.

VAN TONDER, P.J.M & PIENAAR H.C.vZ. 2010. Temperature, water and voltage management on a PEM regenerative fuel cell. *SATNAC.* Paper read at SATNAC congress held in Stellenbosch in September 2010. Stellenbosch.

WENTZEL, M. *Delivering electricity to South Africa's rural areas*. Energy Division, Palmer Development Consulting. February 2004.

ANNEXURES PAGE NUMBERS

ANNEXURE A	Standard Thermodynamic properties of chemical substance	69
ANNEXURE B	Specifications of the Flodos water pump	70
ANNEXURE C	Specifications on the drum type gas meter	73
ANNEXURE D	NEXA Power Module	75

Molecular formula	Name	Δ H (kJ mol $^{-1}$)			Δ G (kJ mol -1)		
		Crys.	Liq.	Gas	Crys.	Liq.	Gas
H_2O	Water		-285.8	-241.8		-237.1	-228.6
H_2O_2	Hydrogen peroxide		-187.8	-136.3		-120.4	-105.6
H_2O_2Sn	Tin(II) hydroxide	-561.1			-491.6		
H_2O_2Sr	Strontium hydroxide	-959.0					
H_2O_2Zn	Zinc hydroxide	-641.9			-553.5		
H_2O_3Si	Metasilicic acid	-1188.7			-1092.4		
H_2O_4S	Sulfuric acid		-814.0			-690.0	
H_2O_4Se	Selenic acid	-530.1					
H_2S	Hydrogen sulfide			-20.6			-33.4
H_2S_2	Hydrogen disulfide		-18.1	15.5			
H_2Se	Hydrogen selenide			29.7			15.9
H_2Sr	Strontium hydride	-180.3					
H_2Te	Hydrogen telluride			99.6			
H_2Th	Thorium hydride	-139.7			-100.0		
H_2Zr	Zirconium(II) hydride	-169.0			-128.8		
H_3N	Ammonia			-45.9			-16.4
H_3NO	Hydroxylamine	-114.2					
H_3O_2P	Hypophosphorous acid	-604.6	-595.4				
H_3O_3P	Phosphorous acid	-964.4					
H_3O_4P	Phosphoric acid	-1284.4	-1271.7		-1124.3	-1123.6	
H_3P	Phosphine			5.4			13.4
H_3Sb	Stibine			145.1			147.8
H_3U	Uranium(III) hydride	-127.2			-72.8		
H_4IN	Ammonium iodide	-201.4			-112.5		
H_4N_2	Hydrazine		50.6	95.4		149.3	159.4
$H_4N_2O_2$	Ammonium nitrite	-256.5					
$H_4N_2O_3$	Ammonium nitrate	-365.6			-183.9		
H_4N_4	Ammonium azide	115.5			274.2		
H_4O_4Si	Orthosilicic acid	-1481.1			-1332.9		
$H_4O_7P_2$	Pyrophosphoric acid	-2241.0	-2231.7				
H_4P_2	Diphosphine		-5.0	20.9			
H_4Si	Silane			34.3			56.9
H_4Sn	Stannane			162.8			188.3
H_5NO	Ammonium hydroxide		-361.2			-254.0	
H_5NO_3S	Ammonium hydrogen sulfite	-768.6					

INNOVATIVE
TECHNOLOGY
WORLDWIDE

MICRO DIAPHRAGM LIQUID PUMPS NF 10 / 11

DATA SHEET E 511

NF 10 KP.51 DC

NF 10 KPDC

NF 11 KPDC

Concept

KNF micro diaphragm liquid pumps are based on the principle of the oscillating displacement pump which is remarkably simple in design. The circular power from the motor is converted into vertical movement by an eccentric. This motion is then transferred to a diaphragm by means of a connecting rod which in conjunction with an inlet and outlet valve creates a pumping action.

NF 10/11 type liquid pumps can be mounted in any position and can deliver up to 0.1 l/min depending on the model and will operate against pressures of up to 10 mWg.

The KNF modular system contains a wide standard range of materials, motors, voltages and frequencies to enable the selection of an optimal solution for your application.

Features

Small and powerful
Micro design and maximum performance resulting from built-in technology are the outstanding characteristics of this product.

Self-priming and excellent for pressure
Sophisticated diaphragm technology and precise valve structures enable performances of up to 3 mWg suction and 10 mWg pressure.

Extreme chemical resistance
The use of chemically resistant materials such as PTFE, PVDF, FFPM or other material combinations for the parts which come in contact with the liquid allows almost all neutral or corrosive liquids to be pumped.

Dry running, durable and maintenance free
The carefully considered design of these pumps allows them to be run dry and ensures safe operation and a long life even under the most severe conditions.

Areas of use

The versatility of KNF pumps allows a wide field of applications to be covered. Over many years our pumps have proved themselves in the following areas:

Analysers
- Medical / pharmaceutical
- Environmental / water treatment
- Food / toxicology

Laboratory
- Filtration
- Chromatography

Cleaning industry
- Cuvette cleaning
- Sterilisers
- Industrial washing machines

Printing
- Ink jet printing
- Photographic / film development

Other applications for diaphragm liquid pumps include: fuel cells, hydrogen generators, CD coating, dental technology, textiles and many more.

Performance Data

Type	Flow rate (l/min)	Suction head (mWg)	Pressure head (mWg)
NF 10/11	0.1	3	10

The KNF Modular Concept of Selection

General note

This Data Sheet provides an overview of the options with our NF 10/11 pumps. Certain standard options will be explained in more detail where necessary.

Flow curves

The flow curves illustrate how the flow rate alters in relation to the pressures before and after the pump. In the case of a combination of both we would be very happy to advise what the expected flow rate would be.

The values given in the curves are dependant upon the liquid, choice of head materials and the type of hoses being used. Therefore a certain deviation is to be expected.
Note: The flow rate is measured with water at 20°C.

1 Materials of head components

KNF FLODOS offers a wide range of different materials for those parts which come in contact with the liquid thus allowing the possibility of pumping most liquids.

2 Motors

E Shaded pole motor (AC)

DC Direct current motor

NF 11 Ironless direct current motor
This provides the following advantages compared to a conventional DC motor: higher durability, less power consumption and smaller size.

DCB Brushless direct current motor
This type of moto has no brushes which can wear down thus giving it a lifetime comparable with an AC motor. (Option with three leads)

3 Voltages / Frequencies

Choose from the different electrical connection possibilities. Special variations are available.

Modules

Our versatile self-selection program allows you to personally determine the optimum characteristics that you require from your pump. Select your diaphragm pump from the following characteristics:

Pump type			
Basic model	Components		
	1	2	3
NF 10/11			

1	Materials of head components	
KP / KP .51*	Head	PP
	Valves	EPDM
	Diaphragm	EPDM
	Resonating diaphragm	EPDM
KV	Head	PP
	Valves	FPM
	Diaphragm	FPM
	Resonating diaphragm	FPM
KT	Head	PP
	Valves	FFPM
	Diaphragm	PTFE
	Resonating diaphragm	FFPM
TV	Head	PVDF
	Valves	FPM
	Diaphragm	FPM
	Resonating diaphragm	FPM
TT	Head	PVDF
	Valves	FFPM
	Diaphragm	PTFE
	Resonating diaphragm	FFPM

* food conform according to the standard NSF/ANSI 169, for further information see options

2	Motoren
E	Shaded pole motor (AC)
DC	Direct current motor
DCB	Brushless direct current motor

3	Voltages / Frequencies
230 V / 50 Hz 115 V / 60 Hz 100 V / 50-60 Hz	for AC motors
6 / 12 / 24V	for DC motors
12 / 24V	for DCB motors

Performance

Basic model	Flow rate at atmos. pressure (l/min)	Max. suction head (mWg)	Max. pressure head (mWg)
NF 10-E	0.1	3	10
NF 10-DC	0.1	3	10

Motor selection	E	DC (NF 10)
Voltage (V)	230V / 50 Hz	6 / 12 / 24
Power rating (W)	9.1	3.8 / 3.7 / 3.4
I Last max. (A)	0.06	0.61/0.28/0.13
I max. (A)	0.08	0.64/0.31/0.14
EMC guideline	EN 55014	EN 55014
Motor protection factor	IP 00	IP 30
Weight	410 g	60 g

Performance

Basic model	Flow rate at atmos. pressure (l/min)	Max. suction head (mWg)	Max. pressure head (mWg)
NF 10-DCB	0.1	3	10
NF 11-DC	0.1	3	10

Motor selection	DCB (NF 10)	DC (NF 11)
Voltage (V)	12 / 24	6 / 12 / 24
Power rating (W)	2.0 / 2.4	2.2 / 2.5 / 2.3
I Last max. (A)	0.17 / 0.1	0.33/0.17/0.08
I max. (A)	0.17 / 0.1	0.37/0.21/0.09
EMC guideline	EN 55011 EN 61000-6-1	EN 55022 EN 55011
Motor protection factor	IP 30	IP 33
Weight	52 g	70 g

NF 10-E

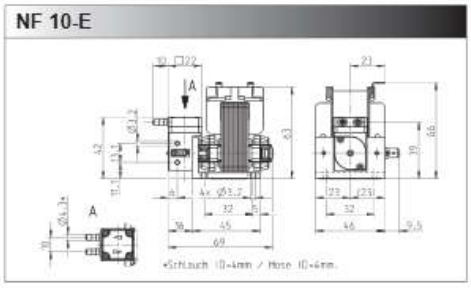

NF 10-DCB

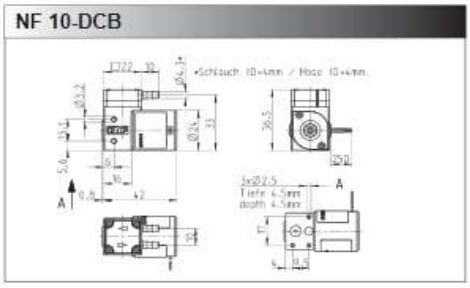

NF 10-DC

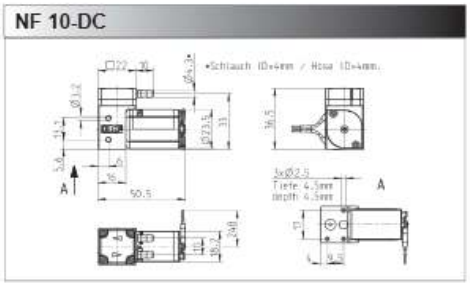

NF 11-DC

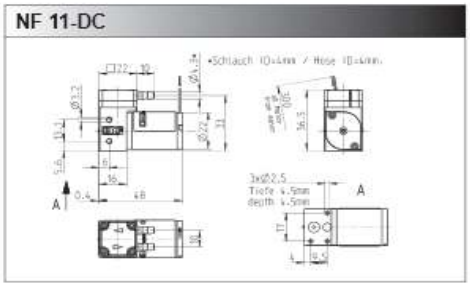

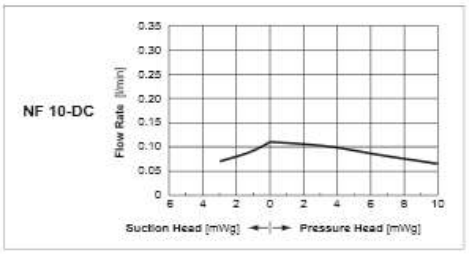

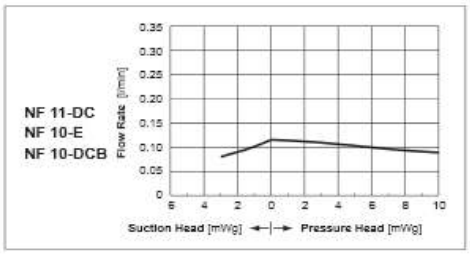

Ritter	**DRUM-TYPE GAS METERS** **Application, Materials** **Series: TG**	**01.03** V 2.0 Rev. 09/2004

TG 1 Model 7
(Fig. with "Totalizing Roller Counter")

RITTER drum-type gas meters are universally applicable for measuring the volume of flowing gases and are particularly effective when measurements demand the highest precision.

The possibility of selecting the gas meter material from among 5 different excellent materials (polyvinyl chloride (PVC), polypropylene (PP), polyvinylide fluoride (PVDF), PE-el (polyethylene electrically conductive) or refined stainless steel 1.4571 (316 L) enables the user individually to meet measurement requirements even in case of highly aggressive gases.

For rugged, industrial applications, robust models with a stainless steel casing and plastic drum (four different materials) are available.

The desired measurement range can be selected from among 9 magnitudes (types) extending as a whole from 0.1 ltr/h to 18,000 ltr/h at a gas temperature ranging from -50 to +120 °Celsius. The solidly manufactured casing of the standard meters is designed to withstand a maximum overpressure of 50 mbar (plastic casings) or 500 mbar (stainless steel casings); meters for higher pressure ranges up to 16 bars are available.

TG 10 Model 5
(Fig. with "Totalizing Roller Counter")

The measurement of **RITTER** drum-type gas meters works on the principle of displacement. The gas meters contain a revolving measuring mechanism (measuring drum) within a packing liquid (usual: water or thin-bodied oil). The measuring drum compulsorily measures volume by periodically filling and emptying four rigid measuring chambers.
Fastidious production methods and calibration enable a measuring accuracy of ± 0.2 % at standard flow rate and approx. ± 0.5% over the whole measuring range.

TG 50
Model 7
(Fig. with "Resettable Roller Counter")

The major advantage and the superiority of volumetric Gas Meters (like Drum-type Gas Meters) over other measurement principles, which determine gas volume using secondary measurable variables such as speed, heat capacity, hot-wire resistance or similar, is that the volume is **directly** measured. That means that the condition and the composition of the gas has no influence on the measurement accuracy.

Correcting factors which take into account gas type, temperature, humidity etc are therefore **not necessary**. It should be noted that with other, non-volumetric measurement processes, the measurement accuracy given for that process can only be achieved if the correcting factors for the immediate condition of the gas are exactly known.

Subject to alterations

Ritter	**DRUM-TYPE GAS METERS** Overview	**01.04** Rev. 03/2010

Standard Equipment:

- 4-Chamber Measuring Drum
- Magnetic Coupling (between the measuring drum and counting mechanism)
- 8-digit Totalizing Roller Counter
- large, one-Needle dial
- Filling-level Indicator (for setting the Packing Liquid level)
- Manometer/Thermometer Supports
- Viton sealing
- Level, and Levelling Feet.

Performance Data:

- Measuring accuracy:
  ± 0.2% at standard flow rate (exact value is stated in individual Calibration Certificate),
  approx ± 0.5% across the measurement range
- Maximum gas inlet pressure (overpressure):
  50 mbar with plastic casings
  500 mbar (0.05 MPa) with stainless steel casings
- Flow rate (measuring range) and meter indication:

Type	Flow Rate			Indication	
	Minimum [ltr/h]	Maximum [ltr/h]	Standard [ltr/h]	Min. Dial Division [ltr]	Maximum Value [ltr]
TG 05	1	60	50	0.002	9,999,999.9
TG 1	2	120	100	0.01	99,999,999
TG 3	6	360	300	0.02	99,999,999
TG 5	10	600	500	0.02	99,999,999
TG 10	20	1,200	1,000	0.1	99,999,999
TG 20	40	4,000	3,200	0.2	999,999,990
TG 25	50	7,000	5,000	0.1	999,999,990
TG 50	100	18,000	10,000	0.5	999,999,990

(1) Indication at EDU32

Available Models (Materials):

Casing	Measuring drum	Model
PVC-transparent	PVC-grey	**5**
PP-grey	PP-grey	**6**
PVDF	PVDF	**7**
PE-el	PE-el	**8**
1.4571 (316 Ti)	PVC-grey	**1**
1.4571 (316 Ti)	PE-el	**2**
1.4571 (316 Ti)	PP-grey	**3**
1.4571 (316 Ti)	PVDF	**4**

Legend:		
PVC	=	Polyvinyl chloride
PP	=	Polypropylene
PVDF	=	Polyvinylide fluoride
PE-el	=	Polyethylene-electrically conductive
1.4571	=	316 Ti
	=	Refined stainless steel
Viton	=	Fluorine rubber

For chemical resistance properties please contact **RITTER**.
Both the casings out of plastic and stainless steel are welded.

Accessories: Thermometer (gas), range 0° to +60°C
Thermometer (packing liquid), range 0° to +60°C
Manometer, range 10 mbar differential pressure
Electronic Display Unit, including Interface RS 232 and Analog Output (requires Pulse Generator)

Built-in Options:
Pulse Generator (for connection of Electronic Display Unit or Computer)
- Standard Version
- Ex-proof Version

High Precision Liquid Level Indicator ("HPLI")
LCD display, resettable, 8-digit (substitutes Totalizing Roller Counter)

Subject to alterations

Fuel Cell Systems & Solutions

Nexa® Power Module

with Integration Kit

Heliocentris presents the Nexa® Power Module by Ballard Power Systems, the world's first volume produced proton exchange membrane fuel cell module.

1200 W | Air Cooled

The Nexa® Power Module comprises an air cooled fuel cell stack using Ballard's approved PEM technology. Consuming hydrogen and oxygen (from ambient air)it generates up to 1200 W of unregulated DC electrical power.

To achieve a complete power module with easy to use interfaces, all necessary auxiliary components are built in: air compressor, cooling fan, humidity exchanger, valves, pressure regulator and microprocessor controller.

The Nexa® Power Module is well-suited for a variety of engineering purposes. The system design enables the integration into a wide range of applications such as

- Stationary power supply systems
- Back-up power generators
- Recreational and portable products.

The Nexa® Power Module comes with a set of start-up components facilitating convenient set-up and integration.

A variety of accessories like hydrogen supply options and power electronics are also available. Please inquire for a customized solution that meets your needs.

heliocentris

www.heliocentris.com

The Integration Concept

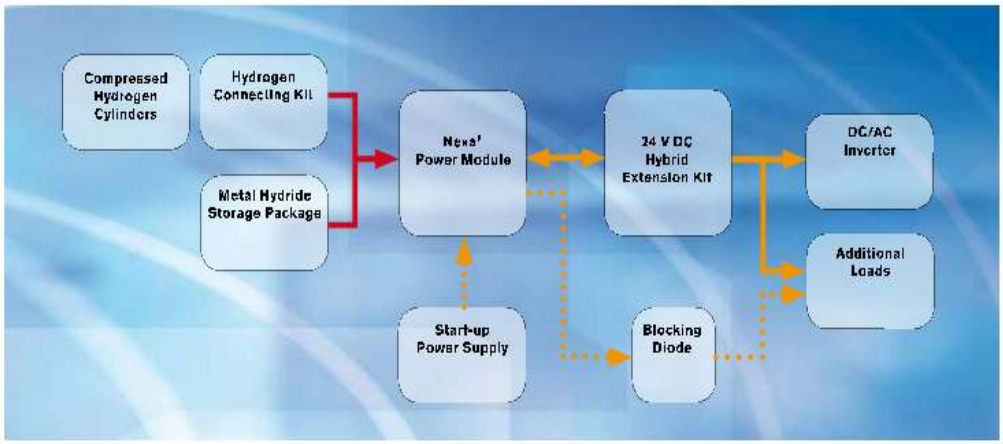

Hybrid Extension Kit

As with all PEM fuel cell systems, the Nexa² Power Module requires an external power source for start-up. Since the fuel cell output voltage varies depending on the current drawn, an additional voltage regulation is necessary.

Our Hybrid Extension Kit is a solution for both requirements. It comprises a DC/DC converter, a rechargeable battery, system control software and all necessary cables.

Custom designed for the Nexa², the DC/DC converter includes a battery charger for hybrid operation as well as back current protection.

Hydrogen Supply Options

Heliocentris offers various solutions for supplying hydrogen to the system.

The most cost effective solution is our Hydrogen Connection Set. Everything is included to take you from the compressed hydrogen cylinder to the Nexa².

The most comfortable solution is our Metal Hydride Storage Package. It comprises a set of 3 HS 900 storage canisters and all necessary tubes and connectors.

The Monitoring Software

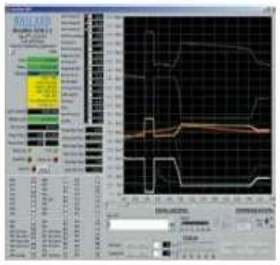

The Nexamon² OEM control software allows the user to set parameters and monitor operational data of more than 20 system variables of the Nexa² Power Module, e.g.

- Stack voltage, current, temperature
- Hydrogen pressure and consumption
- Ambient Temperature
- Air Mass Flow Rate
- System operating time
- ...

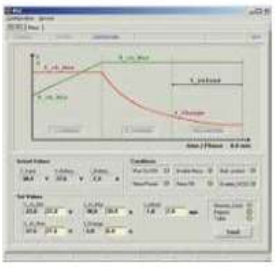

The control software of the Hybrid Extension Kit visualizes all data related to hybridization and battery management. It also allows the user to set different battery types and optimize the charging and discharging parameters.